2023

Investigating Smooth Muscle Myosin Dynamics and Assembly in Physiology and Pathology

Maggie Bennett

LOYOLA UNIVERSITY CHICAGO

INVESTIGATING SMOOTH MUSCLE MYOSIN DYNAMICS AND ASSEMBLY IN PHYSIOLOGY AND PATHOLOGY

A DISSERTATION SUBMITTED TO

THE FACULTY OF THE GRADUATE SCHOOL

IN CANDIDACY FOR THE DEGREE OF

DOCTOR OF PHILOSOPHY

PROGRAM IN CELL & MOLECULAR PHYSIOLOGY

BY

MARGARET BENNETT

CHICAGO, ILLINOIS

AUGUST 2023

ACKNOWLEDGEMENTS

I found this section the hardest to write, because the list feels too long and any words I would write may come up short. So here is my best attempt at a non-exhaustive, I'm sure, list of acknowledgements.

First off I would like to thank my mentor Jordan. When I joined more than four years ago, he was ready to jump in and allow me to branch out and work on a new topic for the lab. My project was based in smooth muscle physiology and pathology, a departure from the world of non-muscle myosins the Beach Lab had known. Motivated by a slightly more clinical application, he helped guide me through what it was like to learn how to work with new cell types, develop new protocols and assays, and to find a niche in a whole new topic. It has not been easy but I have thoroughly enjoyed it along the way. He has been a fearless leader into the unknown world of smooth muscle for the past four years, and his enthusiasm is contagious.

Next, I would like to thank everyone in the Beach and Oakes Labs who have made coming to work feel like going home. Long days filled with imaging and endless western blots were made infinitely better by having each and every one of you there. Each labmate has been kind, helpful, inspiring, and brilliant. I have been so lucky to be surrounded by great scientists, and more importantly, great humans. I’m excited to go back to med school, but will miss you all enormously.

Thank you to my thesis committee. My thesis committee has been extremely helpful in guiding my project. The feedback I've gotten at each committee meeting has pushed my project forward further than I could have on my own. I'm truly grateful for the time and care put in.

The MD/PhD program here at Loyola has been a source of support and inspiration. Without Director Dr. Andrew Dingwall, and former director Dr. Charles Hemenway, I would not be here today and for that I cannot thank them enough.

I'd like to thank my family, and especially my mom for her endless support over the past 6 years and beyond. She has been my sounding board and cheerleader, and the best fake patient I could ask for when I've needed to brush up on clinical skills before an OSCE. To my boyfriend Robbie, thank you for learning more about smooth muscle myosin than any person in commercial real estate should ever know. For helping me in every way you can. And for supporting me through all of the highs and lows that grad school has brought.

TABLE OF CONTENTS

LIST OF TABLES

LIST OF FIGURES

CHAPTER 1

INTRODUCTION

Vascular smooth muscle cells (SMCs) line blood vessels throughout the body, where they dynamically alter vessel diameter to regulate blood pressure, provide structural integrity, and absorb shock on a beat-to-beat timescale. These mechanical and contractile functions are powered by the actin and smooth muscle myosin 2 cytoskeleton. To function, smooth muscle myosin transitions between an inactive monomeric state and an active filamentous state, which can then perform work on actin. Understanding the regulation of smooth muscle myosin activation at the molecular and cellular level is foundational for understanding tissue-level smooth muscle function and dysfunction in disease states. Indeed, mutations in smooth muscle myosin and dysregulation of actomyosin contractility are known drivers of smooth muscle pathologies, such as aortic aneurysms. The overarching goal of this work is to explore filament assembly and dynamics of smooth muscle myosin under normal physiological conditions, and look into how these may be changed in novel and pathology associated mutations.

Smooth muscle is a fundamental component of the cardiovascular system. In major blood vessels, the smooth muscle layer (tunica media) comprises the vast majority of the vessel wall. This medial layer is dominated by vascular smooth muscle cells (SMCs) which are critical to the mechanical functions of blood vessels to provide structural integrity, dynamically contract and relax to alter vessel diameter to modulate blood pressure, and absorb shock on a beat-to-beat

timescale. [1] SMC malfunction results in not only aberrant control of vascular tone and blood pressure, but in catastrophic failure of vascular integrity leading to thoracic aortic aneurysm and dissection (TAAD). [2,3] Nearly 25 percent of TAAD can be attributed to a single gene mutation, with a plurality of those cases driven by mutations in the dominant contractile proteins smooth muscle myosin and smooth muscle actin. [4] To understand how these mutations drive pathology, we must first understand how normal filament assembly and dynamics operate in SMCs.

In this work we analyzed smooth muscle myosin assembly and dynamics during induced contraction. We find that smooth muscle myosin forms highly dynamic filaments at steady state that are stabilized during induced contraction (Aim 1). Furthermore, most smooth muscle myosin is filamentous at steady-state and assembly increases upon induced contraction (Aim 2). This assembly kinetically parallels cytoplasmic calcium release and cell-scale force production. Finally, we find that both a novel mutation and a known pathology associated mutation alter normal assembly and dynamics (Aim 3), indicating that these properties play a vital role in SMC physiology. Therefore, our data supports a model in which SMC forms highly dynamic, but modulatable, filaments. Moreover, activation induces both nascent smooth muscle myosin filament formation and activation of pre-existing filaments. Both of these phenomena are altered in mutations along the tail region of smooth muscle myosin.

Specific Aim 1: Determine stability and dynamics of smooth muscle myosin filaments at steady state and during activation.

- Perform FRAP under a variety of conditions to determine monomeric exchange within smooth muscle myosin filaments before and after induced contractility

Specific Aim 2: Examine fraction of smooth muscle myosin in filamentous form and monomeric form at steady state and following activation.

- Develop and utilize a single cell image-based assembly assay to measure fraction of filamentous myosin.

Specific Aim 3: Investigate how MYH11 mutations may affect filament assembly and dynamics.

- Examine the impact of both novel mutations and known pathology associated mutations on the assembly and dynamics using imaging-based assembly assays and FRAP.

Impact: By furthering our understanding of smooth muscle myosin, we can shed light onto molecular mechanisms behind a fundamental physiological tissue. In understanding smooth muscle myosin dynamics, we can better understand smooth muscle contraction. With this knowledge, we can probe changes in filament assembly and dynamics in disease causing mutations and better understand devastating cardiovascular disease like aortic dissection.

CHAPTER TWO

REVIEW OF LITERATURE

Smooth Muscle Overview

Smooth muscle surrounds many hollow organs throughout the body, playing a vital role in human physiology. By surrounding these organs, smooth muscle produces contractions that dynamically modulate the organ diameter, leading to a variety of organ-dependent functions. For instance, smooth muscle contraction moves food along the digestive tract, modulates pressure in the eye, expels urine from the bladder, and is responsible for uterine contractions during labor and childbirth. Smooth muscle function is imperative for carrying out normal body physiology as a whole. In fact, without viable smooth muscle, mice experienced incomplete emptying leading to distended bladders and gastrointestinal issues resulting in mortality as neonates. [5] This emphasizes that smooth muscle, specifically its functional and regulated contraction, is essential to human life.

While smooth muscle is a type of muscle, it differs from skeletal or striated muscle in organization, function, and regulation. One of these significant differences is the neural regulation of contraction. Smooth muscle contraction is involuntary, meaning we have no control over the timing, presence, or duration of contraction. In contrast, we have voluntary control over skeletal muscle; meaning if we want to kick our leg or flex our arms, we are capable of controlling the timing, the strength, and the duration of contraction. Because this is not the case in smooth muscle, smooth muscle contraction, and therefore blood pressure regulation, airway

tone, peristalsis of food through the GI tract, and all the other effects of smooth muscle contraction, exist outside conscious control. Smooth muscle contraction is a silent regulator of human physiology keeping us alive.

Vascular Smooth Muscle is an Integral Component of the Cardiovascular System

While smooth muscle acts in nearly all areas of the body, a particularly interesting type is vascular smooth muscle. Smooth muscle surrounds many arteries and through varying degrees of tonic contraction helps regulate blood flow, blood pressure, and contributes to vessel integrity throughout the body.

Muscular arteries are composed of three layers–the intima, the tunica media, and the adventitia. Each of these layers serves a unique purpose. The intima is composed primarily of a monolayer of endothelial cells which help form a barrier between blood, surrounding tissue, and the rest of the blood vessel. Additionally, they play a role in regulating the coagulation cascade and vessel tone. [6] The middle layer or tunica media is the thickest layer and is dominated by vascular smooth muscle cells (VSMCs) which are critical to the mechanical and structural functions of blood vessels. In major blood vessels, the smooth muscle layer comprises the vast majority of the vessel wall. It allows the vessels to dynamically contract and relax to modulate blood pressure by altering afterload and allows the aorta to absorb shock from high velocity blood coming from the left ventricle on a beat-to-beat timescale. [6] Finally, the outermost layer of the blood vessel is the adventitia. The adventitia is composed mainly of connective tissue, nerves, and the vaso vasorum, the latter helping to supply oxygen and nutrients to the vessel. [7] The function of each of these layers in concert creates dynamic and responsive vessels capable of transporting blood and nutrients within arteries and veins and throughout the body.

The timing, magnitude, and duration of smooth muscle cell contraction and force is tightly regulated. An abnormal increase in smooth muscle tone, due to increased smooth muscle cell mass (by hypertrophy, hyperplasia, or both) or hypercontractile smooth muscle cells is implicated in the pathophysiology of a variety of diseases. Specifically, hypercontractile VSMCs can increase afterload causing high blood pressure which when left unchecked can result in stroke, kidney failure, heart failure, or other issues. [8] Hypercontractile SMC are implicated in the pathophysiology of asthma as the airway is narrowed more quickly and more robustly than in airways without hypercontractile SMC. [9] If an increase in smooth muscle mass occurs in the uterus, the uterus can become hypercontractile and uterine myomas can be present affecting fertility and causing pain. [10] Each of these examples illustrates that generating and maintaining the appropriate level of contraction is key to healthy organ function throughout the body.

Smooth Muscle Cell Phenotypes

Vascular smooth muscle cells have to be able to provide tonic contraction within the vessel, as well as be able to migrate and divide to respond to trauma or injury. To do both of these different tasks, smooth muscle cells exist in two phenotypes - synthetic and contractile. However, rather than being a strictly binary system, there is a continuum between synthetic and contractile that many cells exist alone. The synthetic phenotype is highly proliferative, migratory, and synthesizes large quantities of matrix proteins. [11,12] The contractile phenotype is capable of greater force production as it expresses more contractile proteins. [13] The contractile phenotype is often referred to as the more differentiated phenotype, however it retains a high degree of plasticity. Smooth muscle cells in the contractile phenotype are capable of downregulating contractile proteins and switching to the synthetic phenotype in response to

extracellular environments or cues. This phenomenon of phenotype switching was originally described by Chamley et al. in the 1970s, and has remained a topic of interest. [14] Phenotype switching can occur after vascular injury and, at least in early stages, is reversible. [15]

Synthetic Phenotype

The synthetic phenotype is often implicated in pathophysiology. The synthetic phenotype is considered a less differentiated phenotype, as the cells decrease contractile protein expression while increasing the synthesis of matrix proteins. When this phenotypic switch of smooth muscle cells occurs and persists within the vasculature, atherosclerotic plaques can form. [16,17] In response to an insult, inflammatory changes result in synthetic SMCs conglomerating with inflammatory cells to form a plaque. If intervention occurs early enough, this phenotype switch is reversible and synthetic SMCs can become a more contractile phenotype again. As an increasing number of contractile cells revert to synthetic within the blood vessel, contraction of the vessel is compromised and the diameter of the lumen is shrunk. This creates smaller, less efficient vessels and overlying fragile plaques capable of detaching at any time. The majority of cases of sudden cardiac ischemic deaths are the result of these plaques rupturing and causing sudden thrombosis and vessel occlusion. [18] Therefore, while transient phenotype switching is important for migration and wound heading, switching from a contractile phenotype to a persistent synthetic phenotype within the blood vessel is a potentially deadly effect.

Contractile Phenotype

As mentioned above, the contractile phenotype is the fully differentiated phenotype with high expression of smooth muscle actin and myosin allowing for force production at a variety of lengths. In healthy blood vessels, nearly all SMCs are in the contractile phenotype.

The fact that VSMC phenotypes exist along a reversible spectrum is highly relevant to research because SMCs in culture tend to dedifferentiate into a more synthetic phenotype. Because contractile VSMCs are terminally differentiated and largely nonproliferative, they are difficult to maintain in culture. Therefore, cells cultured for research tend not to be purely contractile. Protocols that induce cells towards a contractile phenotype, and using primary cells at low passage number can both increase the level of contractile cells present in any given experiment.

Smooth Muscle Contraction - Contractile Proteins

Contractile Unit

Force achieved by smooth muscle cells is a result of smooth muscle myosin 2 acting on the actin cytoskeleton, utilizing the sliding filament model first described by Huxley and Hanson. [19–21] This system of large myosin networks acting in concert on actin to produce cell level force is similar to other muscle contraction throughout the body, utilizing the same basic system as skeletal muscle and cardiac muscle albeit with different myosins. In skeletal muscle, skeletal muscle myosin and actin within a sarcomere produce contraction. While unique, both these myosins do share some characteristics. Smooth muscle myosin is a member of the myosin 2 family, which also consists of striated myosin 2s (skeletal and cardiac) and non-muscle myosin 2s (NM2). [22]

Smooth Muscle Myosin

All myosin 2 “monomers” are heterohexamers that form the basic assembly unit of myosin filaments. The tail of each monomer can reversibly associate with other monomers in parallel and antiparallel fashion to drive assembly of bipolar filaments [23], placing motor

domains at opposing ends. These filaments are the functional unit of the myosin that interact with filamentous actin to drive contractile events.

Smooth Muscle Actin

Smooth muscle actin is the structural element of smooth muscle cell cytoskeleton which provides structural integrity and helps transmit force produced by smooth muscle myosin throughout the cell and ultimately tissue. The actin in the cell exists in two main populations and can be divided into contractile actin and cortical actin. Contractile smooth muscle actin forms the thin filaments in smooth muscle, surrounding myosin and providing a substrate for the myosin motor to exert work. Cortical smooth muscle actin spans the cell cortex and attaches to the plasma membrane at dense plaques. At these dense plaques, linker proteins connect transmembrane integrins to actin filaments to transmit force from within the cell to the extracellular matrix and neighboring cells. [24]

Not only does actin provide a structure for the dynamic smooth muscle myosin, but smooth muscle actin filaments themselves are dynamic as well. Like myosin, actin filaments can be assembled and disassembled with contraction and relaxation, and altered in disease. For instance, in the airways of asthmatics, the smooth muscle has increased actin filament formation and contractile capacity. [25] Overall, research has indicated that actin filaments in SMCs are dynamic within the short term and long term disease states.

Smooth Muscle Contraction - Mechanisms of Contraction

While the force produced by SMC contraction is mechanically performed by smooth muscle myosin and actin, cytosolic calcium levels regulate the production of force. Smooth muscle cell contraction is contingent upon calcium dependent regulatory light chain

phosphorylation which leads to the formation of crossbridges between smooth muscle myosin and actin. The details of how, when, and why this happens has been a source of investigation for decades. Broadly speaking, increase in cytosolic Ca2+ binds calmodulin, activating myosin light chain kinase, which phosphorylates the light chain of myosin, and activates myosin producing contraction.

Calcium Cascade

Calcium has been implicated in muscle contraction and relaxation for nearly 150 years, with Ringer first observing that isolated hearts beat more robustly and for longer when bathed in a solution containing calcium.[26] Smooth muscle operates similar to cardiac muscle in this regard, and the presence of calcium is the main instigator of efficient contraction.

In response to an agonist, calcium is increased in the cytoplasm, either by Ca2+ influx from the extracellular space or by Ca2+ movement from the sarcoplasmic reticulum into the cytosol. Ca2+ concentrations both in the extracellular space and the sarcoplasmic reticulum are several fold higher than in the cytosol, so as channels open on both the plasma membrane and SR membrane Ca2+ flows down its gradient, out of those reservoirs, and into the cytosol. [27]

Both sources of Ca2+ release from the sarcoplasmic reticulum and influx of Ca2+ from the extracellular space are important for SMC contraction. However, smooth muscle can contract in the absence of extracellular Ca2+, as the sarcoplasmic reticulum holds enough Ca2+ inside that release of stores sufficiently binds to CaM and activates MLCK to produce contraction. [28]

Ca2+ release from the SR can be stimulated through agonist-receptor interaction and the

IP3 pathway. An external agonist binds a receptor on the cell's plasma membrane, activating phospholipase C (PLC) which breaks down PIP2 into IP3.[29] IP3 then rapidly diffuses through the cytosol, binding to receptors on the SR, and stimulating Ca2+ release from the SR into the cytosol. The importance of this pathway's significance in facilitating smooth muscle contraction has been demonstrated in the IP3 KO mouse model. In the smooth muscle specific IP3 knockout mouse, aortic contraction and blood pressure were decreased in response to a myriad of activators, indicating powerful VSMC contraction could not be produced.[30]

Within smooth muscle cells, cytosolic free Ca2+ contributes to contraction through Ca2+ - dependent regulatory light chain (RLC) phosphorylation. Free Ca2+ in the cytosol binds calmodulin (CaM), CaM then activates myosin light chain kinase (MLCK). MLCK phosphorylates the light chain of myosin, which facilitates the mechanical interaction of smooth muscle myosin and actin resulting in contraction. \cite{De_Lanerolle1980-if}\cite{De_Lanerolle1982-fk} The converse is also true. Smooth muscle relaxation occurs as this process is essentially reversed. Sequestration of Ca2+ back into the sarcoplasmic reticulum and extracellular space causes a decrease in cytosolic calcium, light chain phosphorylation, and ultimately, muscle tone. [31]

Activators

Extracellular calcium can enter the cytoplasm and trigger smooth muscle contraction in response to membrane depolarization, hormone stimulation or neurotransmitter stimulation. [32] Smooth muscle cells can be activated in a myriad of different ways. Activation causes an increase in intracellular calcium release and subsequent contraction. By being able to respond to a variety of cues, smooth muscle contraction is highly regulated. It can be regulated by tissue, by

time, and by method of activation producing specific responses throughout the body. Two such activators are carbachol and angiotensin II, both of which are used in our research.

Class 2 Myosin Overview

Class 2 Myosin Family

Smooth muscle myosin belongs to a larger class of myosins, called the conventional class 2 myosins. These myosins include striated myosins (cardiac, fast and slow skeletal myosins, ocular myosins, etc.) on one branch and smooth and non-muscle myosins on the other. [33] While all related, non-muscle and smooth muscle myosins are more closely related genetically and phylogenetically than smooth is to straited .

All class 2 myosins have a number of things in common. They all consist of four main domains–a globular motor domain, a neck domain, a coiled-coil tail domain, and a nonhelical tail piece. [22] The globular motor domain allows each myosin to interact with and act on actin, using the power stroke to create force. The neck domain serves as a converter, translating power produced and protein conformational changes from the motor domain down through the tail. The coiled-coil tail domain allows for each myosin monomer to associate with other monomers to form filaments.

Understanding smooth muscle myosin in the larger context of related and class 2 myosins is significant because it allows for the examination of the similarities and amplification of the differences in smooth muscle myosin.

Non-muscle Myosin in Smooth Muscle

While smooth muscle myosin is the most abundant class 2 myosin in smooth muscle, another class 2 myosin, non-muscle myosin 2A (NM2A), also plays a role in contraction. NM2A

makes up a significant amount of the myosin in smooth muscle cells throughout development. While evolving over the course of life and present in various tissues, NM2 is found to compose 67\% of smooth muscle myosin in the human neonate and adult lungs, and while lower in the aorta, significant amount of NM2A are still present. [34,35] Not only is NM2A present, but it plays an integral role in SMC contraction. In fact, smooth muscle without smooth muscle myosin can contract, primarily due to the contributions of NM2A.[36,37] It was found that NM2A remained phosphorylated after smooth muscle myosin during contractions, indicating NM2A may play a role in SMC ability to sustain contraction. [38] NM2A is also thought to aid in adhesome assembly and force transduction. [39] In disease states, non-muscle myosin 2A regulates aortic stiffness by affecting focal adhesions within SMCs and the cortical cytoskeleton. [40] Overall, research has proved that, while not the most highly expressed myosin, non-muscle myosin plays a significant role in SMC physiology and pathophysiology.

Smooth Muscle Myosin

Smooth muscle myosin, the main myosin expressed in SMCs, exists as a heterohexamer made of two heavy chains, two essential light chains, and two regulatory light chains. The heavy chain is about 200 kDa, the essential light chain is 17 kDa and the regulatory light chain is 20 kDa. Each of these is noncovalently bonded to the heavy chain. The heavy chain itself can be divided into four main regions: the motor, the neck, the coiled-coil tail, and non-helical tailpiece.

Motor and Neck Domains

The motor head of smooth muscle myosin is, as named, responsible for force production. The head is made of a globular motor domain, a small folded domain called the converter, and a regulatory domain of a long alpha helix that has binding sites for the light chains. [41] When the

myosin motor head binds to actin, ATP is hydrolyzed resulting in a conformational change of the myosin, altering its affinity to actin, which together causes myosin to produce a power stroke and pull on the actin, generating force. [42]

The light chains binding help to stabilize and stiffen the converter region and allow it to amplify small conformational changes into a working production. [43] Altogether, these domains are formed by about the first ~850 residues of the heavy chain and help produce the power stroke.

Tail Region: Coiled-Coil

Following the neck region is the tail of smooth muscle myosin. Each heavy chain tail consists of an alph-helix that dimerizes into a coiled-coil via a canonical heptad repeat. The heavy chain is an alpha-helix heptad repeat that dimerizes into a coiled-coil tail. Along this rod intermittent hydrophobic residues are present. [44] This repeating alpha helix allows for myosin monomers to interact with other monomers to form filaments. [45] This tail region allows for the formation of bipolar filaments or side polar filaments. Importantly, changes or mutations along the tail can impact myosin's ability to form filaments and it's ability to fold into the compacted monomeric state. [46]

Structural States

Smooth muscle myosin can exist in multiple states. First, monomers can exist in a folded, inactive state, termed 10S, or an unfolded assembly-competent state, termed 6S. [47–49] The folded 10S autoinhibited state has two key structural features: (1) the coiled-coil tail folds twice to wrap around the motor domains and stabilize the inhibited monomer; (2) the formation of the interacting heads motif (IHM), in which the motor domains dock on one another and fold back

onto the N-terminus of the coiled-coil tail, thus preventing actin binding and ATP hydrolysis. The IHM and folded tail are not obligate, as the IHM has been observed and explored in filamentous striated muscle myosin 2s where it creates a partially-active (or partially-inactive) filament. Here, the IHM is the likely structural basis of the low energy super relaxed state (SRX) [50,51] but this filamentous IHM/SRX state has not been clearly demonstrated for SM2 or NM2 in cells.

Finally, to drive contraction, all myosin 2s can enter the open and active filamentous state. For smooth myscle myosin and NM2, the conversion from the folded inactive 10S to the assembly-competent 6S is largely dependent on the phosphorylation of key residues on the regulatory light chain (RLC) [52–54], which can be phosphorylated by calcium-mediated activation of myosin light chain kinase (MLCK). [55–57]

Smooth Muscle Isoform Definition

All smooth muscle myosin is generated from a single MYH11 gene. Two RNA splice events produce four unique protein isoforms, termed SM1A, SM1B, SM2A, and SM2B. SM2 isoforms have a shortened non-helical tail (9 amino acid carboxy terminus) versus the longer variant on the SM1 tail (43 amino acid carboxy terminus). [58] SM-B isoforms have a seven amino acid insert in the motor domain that is absent from SM-A isoforms. [59] These two splicing events appear uncoupled from one another, thus combining to generate four unique polypeptides. Each of these isoforms are illustrated in the Figure 1.

Figure 1. Schematic Illustration of Smooth Muscle Myosin Isoforms and Splice Variants. The four isoforms of smooth muscle myosin are displayed. SM1A has the extended tail but no motor insert. SM1B has both extended tail and motor insert. SM2A has neither extended tail nor motor insert. SM2B has the motor insert but not extended tail.

Isoform Expression Variation

In normal physiology, different smooth muscle myosin isoforms are dominant in various organs, and in disease states, abnormal isoforms appear, breaking from trend. There are both phasic and tonic smooth muscles.[60] While phasic smooth muscle contracts and relaxes in waves with short and rapid peaks of contraction, tonic smooth muscle contracts for longer periods of time and relaxes while maintaining a high basal level of tone. SM-B isoform is elevated in smooth muscles exhibiting phasic contraction, like bladder smooth muscle or gut smooth muscle.[61] While SM-A isoform is the predominant isoform of smooth muscle cells with tonic contraction, like vascular smooth muscle cells. [62]

While SM-A and SM-B isoforms differ in their motor regions, they also differ in ATPase activity. The SM-B isoform, which has the motor domain insert, also has about two fold greater

ATPase activity compared to the SM-A isoform. [63]This has physiological consequences, as SM-B isoforms appear overexpressed in the lungs of asthmatics, and SM-B isoforms may be producing faster, stronger bronchoconstriction, contributing to disease. [64] Interestingly, this expression is plastic and SM-B isoforms are found to be downregulated in asthmatic equines treated with corticosteroids. [65] This highlights differences between isoforms and the importance of regulating their expression.

The functional consequences of the lengthened non-helical tail region in the SM1 isoform compared to the SM2 isoform is not fully understood. However, studies that have removed the tail extension suggest that the region may be important for regulating filament assembly and homeostasis between filament formation and 6s or folded formation. [66]

While each isoform is unique and tends to be expressed dominantly in certain tissues, expression is not binary. In fact, it has been shown that in many cells, multiple isoforms are expressed. [67] This diversity in expression gives smooth muscle cells a wide variation of filament assembly properties, ATPase activity, and overall contractile properties possibly. This allows smooth muscle to meet the organ dependent demands throughout the body.

Smooth Muscle Myosin Filaments

Filament formation

Filament formation occurs by electrostatic interactions between smooth muscle myosin monomers along the coiled-coil region. The variety of ways each monomer can interact with each other along this tail region allows for multiple staggered myosins to stack on top of each other, forming filaments.

Filament structure

The exact structure of smooth muscle myosin filaments has eluded the field for decades. While this question has been definitively answered for many other myosins, including non muscle and skeletal muscle myosin. However, in smooth muscle the debate continues on between two agreed upon possibilities: a bipolar filament and a side polar filament. There is evidence for both smooth muscle myosin bipolar and side polar filaments in vitro. Bipolar filaments have SMM monomers which interact via parallel and antiparallel interactions along the alpha helical tail region. Interestingly, which of these plays a physiological role in contraction at the tissue level remains undecided.

Various class 2 myosins, non-muscle myosin and cardiac, are known to form bipolar filaments with a central bare zone. The same has been seen in smooth muscle myosin as purified smooth muscle myosin monomers have been shown to form bipolar filaments in numerous studies. [68–70]

There is also evidence for side polar filament structure which has been seen in isolated smooth muscle cells examined with electron microscopy. [71,72] In the side polar filament, the crossbridges have a non-helical arrangement and their polarity is the same on one side of the filament and the opposite along the opposite side. This structure has been proposed to explain how smooth muscle contracts to a smaller size compared to initial size when compared to striated muscle.

Smooth muscle myosin filaments are much less stable than striated muscle myosin filaments, but filament formation can be stabilized by different cellular conditions or proteins. One stabilizing protein is caldesmon. Caldesmon was found to crosslink actin and myosin and stabilize formation of smooth muscle myosin filaments. However, this effect was disturbed by

the presence of calmodulin. [73]

Isoform Heterofilaments

There has been debate over which isoforms of myosin, and how many, are present in a filament. While different isoforms dominate different tissues, there is often a mixture of isoforms present in tissues and cells. This raises the possibility of multiple isoforms being present within a single filament. There is conflicting evidence on the possibility of heterofilaments made up of multiple different isoforms. Kelley et al., found no evidence of heterofilaments, and instead found single isoforms forming filaments with each other.[74] However, Tsao et al., found evidence of SM1, SM2, and SM1-SM2 filaments, indicating that heterofilaments exist. [75] Together, this reveals the picture of heterofilament formation is complex and an unsettled debate.

Additionally, our work indicates that non-muscle myosin and smooth muscle myosin may be capable of co-assembling and forming heterofilaments. This has not previously been seen, and opens an entire new door into what a heterofilament may be composed of.

Filament Response to Contraction

Smooth muscle has a remarkable capability to adapt and contract at different lengths. For instance, the smooth muscle in the bladder may be stretched as the bladder fills before contracting to empty the bladder. Similarly, the vascular smooth muscle cells in the aorta are stretched with each heartbeat, and yet are able to contract against this pressure. It is believed that, in order to accomplish this, smooth muscle builds contractile units in series.[76] This feature suggests the network of contractile units may be flexible and able to be assembled and disassembled dynamically.

Filament formation has been studied in response to activation or contractile stimulus. To study filament formation upon activation, bifirengence was measured in pig tracheal smooth muscle after activation. It was found that bifirengence increases, suggesting filament thickening which suggests that while a portion of SMM remains consistently filamentous, some portions of SMM may form filaments during contraction and dissociate during relaxation. [77] This is an important distinction with striated muscle. Where striated muscle is entirely dependent on the activation of existing filaments to produce contraction, smooth muscle may be using a combination of existing filaments and new filaments.

In this way, smooth muscle myosin polymerization mirrors actin polymerization. Both the contractile proteins appear to form dynamic networks that can, at least to some extent, be broken down and built up in response to stimulus or cellular activity. Actin polymerization has been shown to increase after stimulation of VSMCs. [78] Overall, provided the length and time scales of contraction required for smooth muscle throughout the body, it makes sense that the molecular machinery driving those contractions possess dynamic assembly properties that parallel the physiology. In this way, smooth muscle sets itself apart from other muscle types and makes for a fascinating system to study.

Filament Regulation

The activity of filaments is primarily regulated through phosphorylation of the regulatory light chain. As mentioned previously, smooth muscle myosins can be in a “shutdown” state with the activity of myosin suppressed by asymmetric interactions between the heads. Unphosphorylated smooth muscle myosin is unable to perform work on actin.[79,80] This allowed smooth muscle myosin to oscillate between relaxed and contracting. Work by the

Trybus lab indicated that only one regulatory light chain needs to be phosphorylated to interrupt this shutdown state and activate myosin. [81,82]

Smooth Muscle Myosin Dynamics

Myosin 2 Dynamics: NM2, SKMM, SMM

Myosin 2 family members display disparate polymer exchange kinetics (the equilibrium between monomer and filament) and monomer:polymer ratios (total myosin 2 in monomer or filament at any given time). Figure 2.2 illustrates myosin dynamics as monomer is incorporated and released from the filament. For example, non-muscle cells dynamically modulate non-muscle myosin 2 (NM2) filament assembly to control where and when they generate contractile force while maintaining about half of the total myosin 2 pool in filamentous form. [83,84] In contrast, striated myosin 2s assemble more stable filaments that generate contractile force independent of new filament assembly, with the vast majority of the total myosin 2 pool in filamentous form. [85]

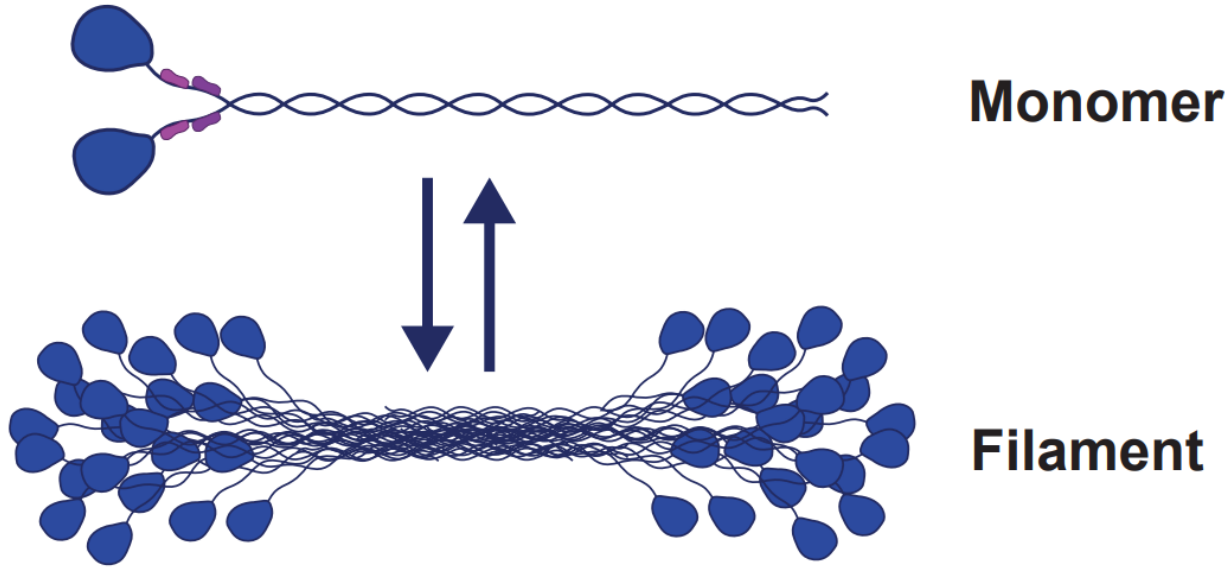

Figure 2. Smooth Muscle Myosin Monomer Exchange within a Filament. Turnover can occur as proteins are synthesized and degraded. However a faster and more rapid exchange of myosin can occur within filaments as monomers are integrated into and leave filaments. We refer to this equilibrium between monomer and polymer as filament exchange kinetics.

Surprisingly, we do not know how smooth muscle cells modulate smooth muscle assembly and activation to generate contractile force, although there is a stated assumption that SMC contractility is driven by activation of pre-assembled smooth muscle myosin filaments. [86] Considering smooth muscle myosin is genetically similar to non-muscle myosin 2 but perhaps more functionally similar to striated myosin 2s where it drives repeated uniaxial contractile events, how smooth muscle myosin will behave in cells is difficult to predict without experimentation.

TAAD Pathophysiology

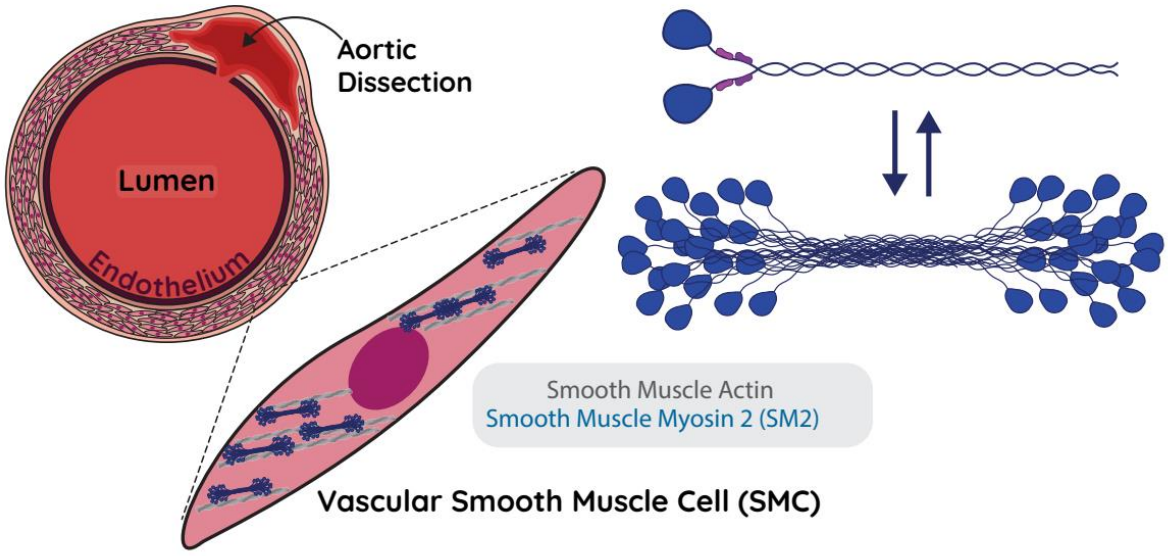

Figure 3. Smooth Muscle Contractility Aids in Aortic Aneurysm and Dissection Prevention. Smooth muscle myosin monomers form filaments which interact with and act on actin to produce force. This force provides structural stability to the blood vessel. Without proper support, blood vessels can balloon out producing an aneurysm or even dissection.

Overview

SMC malfunction results in not only aberrant control of vascular tone and blood pressure, but in catastrophic failure of vascular integrity leading to thoracic aortic aneurysm and dissection (TAAD). [2,3] A thoracic aneurysm occurs when changes in the blood vessel integrity result in a permanent and localized dilation of the artery. A thoracic aneurysm predisposes the patient to thoracic aortic dissection. Dissection occurs when blood tears through the layers of the vascular wall, and blood flows from the lumen into the media. This is an emergent and potential deadly occurrence, as the patient is essentially bleeding internally.

Dissection is a fast moving, and often lethal event, and can be unpredictable. Patients present with a sharp, tearing chest pain, abnormal pulses, and often an impending sense of doom.

When caught early enough, dissection can be treated surgically. However, it is often difficult to get the patient to the hospital, evaluate, and operate in time. [4] Up to 50\% of individuals who experience a type A aortic dissection (a dissection of the ascending aorta) caused sudden death.[87] Therefore, a deeper understanding of the contributing causes to TAAD is needed.

Nearly 25\% of TAAD can be attributed to a single gene mutation, with many of those cases driven by mutations in the dominant contractile proteins smooth muscle myosin 2 and smooth muscle actin.[4] While much research has been done about the effect of connective tissues diseases, like Marfan Syndrome, less is known about how contractile protein mutations contribute. Both smooth muscle myosin and smooth muscle actin mutations have been implicated in disease indicating that interfering with the contractile apparatus of VSMCs in a variety of ways can cause disease. This concecpt is illutated in Figure 2.3.

MYH11 mutations are known to be associated with and/or cause TAAD. While different mutations may have different effects, an analysis of multiple patients and mutations found that the average age of dissection in patients with MYH11 mutations was 44 years old. [3] This indicates that while age may increase risk for aortic aneurysm and dissection, these mutations are compromising vascular integrity decades sooner than aging alone. Both age and mutations may impair the aorta's ability to act as a shock absorber, and leave the vessel susceptible to damage. [88] This could occur as smooth muscle becomes hypocontractile or hypercontractile. If SMCs became hypocontractile due to a mutation in myosin altering force production, the aorta would be too weak to contract against the force of the blood coming from the heart. If smooth muscle myosin mutations left SMCs hypercontractile, increased vascular tone may result in stiffening of the tissue, impairing its ability to absorb force produced as blood is pumped against the vessel

wall.

MYH11 mutations have been reported in the literature in a variety of case studies. Mutations in the tail region of the protein have been shown to increase aortic stiffness, even in individuals who do not have measurable aortic aneurysm.[89] MYH11 mutations have been seen in cases of familial history of TAAD. [90,91] Not only have cases of MYH11 mutations contributing to aneurysm been found in the aorta of adults, but there have also been case reports of infants experiencing aneurysms elsewhere in the body. [92,93]

Models to Study Smooth Muscle

Mouse

The ideal method to study smooth muscle is in intact tissues, most easily done in rodents. Mouse and rat studies have been enormously helpful in elucidating tissue response to stimuli, teasing out factors that impact blood pressure, among many other important questions in the smooth muscle field. [94–96] However, no mouse exists with a fluorescently tagged smooth muscle myosin heavy chain, and because of this, mouse studies are impossible for our research. While creating such a mouse is a high priority for our lab, within the timescale of my research it was not feasible. Therefore, I have turned to cell lines to answer foundational questions about smooth muscle cell biology.

Cell lines

There are many cell lines to study smooth muscle principles. The A7R5 cell line, isolated from the rat aorta, was created and characterized by the mid 1970s, and for decades has played a role in critical investigations into smooth muscle cell physiology. [97] There are over 1,000 citations for this cell line, according to the ATCC website. So while not an in situ model, this cell

line has been highly validated and used throughout the field. Another common method of smooth muscle research in cells is to use primary cells. There are a variety primary cells available, including uterine, airway, and vascular smooth muscle cells. The vascular smooth muscle cells are isolated from human adult aortas without disease, but further information is limited. It is these primary human vascular smooth muscle cells, along with the A7R5 cell line, that I have used.

CHAPTER 3

SMOOTH MUSCLE MYOSIN FILAMENT DYNAMICS

Materials and Methods

Mammalian Expression Vectors

To make pEGFP-SM1A, a single gBlock was purchased from IDT that contained the 5' 420 basepairs of human SM1A, including the naturally occurring Sal1 restriction site, a short 5 basepair linker to facilitate restriction enzyme digestion, and the terminal 3' 616 base pairs, including the naturally occurring Blp1 restriction site and a terminal stop codon. This dsDNA was inserted into pEGFP-C1 after digestion with Bgl2 and Kpn1 restriction enzymes. The internal coding sequence of MYH11 not included in the gBlock was digested from full-length cDNA (MHS6278-202857900; Horizon Discovery) with Sal1 and Blp1 (4911 basepairs) and ligated into the pEGFP-C1-SM1A intermediate following digestion with Sal1 and Blp1.

To make pLVX-GCaMP7s, jGCaMP7s was PCR amplified from pGP-CMV-jGCaMP7s (Addgene \#104463). Following gel extraction, this dsDNA was inserted into the pLVX backbone with a CMV promoter using Gibson Assembly. GCaMP7s subject to PCR was sequence validated. Non-muscle myosin 2A-mApple was described previously. [98]

Antibodies Used and Concentrations

Table 1. Antibodies Used and Concentrations

Protein	Company	Catalog Num	Technique	Concentration
Smooth muscle myosin	Abclonal	A4064	WB	1:1000
Smooth muscle actin	Abclonal	A17910	WB	1:1000
GFP	Santa Cruz	SC-9996	WB	1:1000

Cell Culture and Transfection

Rat aortic smooth muscle cell line, A7R5 cells, were obtained from ATCC and cultured in DMEM (MT10013CV, Corning) supplemented with 10\% fetal bovine serum (MT35-010-CV, Corning) and 1\% antibiotic–antimycotic solution (MT30004CI, Corning). At 24 hours prior to each experiment, A7R5 cells were transfected with 2 ug total DNA using the lipid based transfection system LipoD 293 DNA transfection reagent (SignaGen, catalog #\ SL100668). The A7R5 cells used for traction force microscopy were treated with lentivirus expressing GCaMP7s. A GCaMP7s positive population was obtained using fluorescence activated cell sorting. Lentiviral production was performed in HEK-293-FT cells using psPAX.2 and pMD2.G with LipoD 293 DNA transfection reagent. Lentiviral-containing media was collected at 48 and 72 hrs, filtered, and directly used for transformation of A7R5 cells. Plasmid psPAX2 was a gift from Didier Trono (Addgene plasmid # 12260 ; http://n2t.net/addgene:12260 ; RRID:Addgene 12260)

and pMD2.G was a gift from Didier Trono (Addgene plasmid # 12259 ; http://n2t.net/addgene:12259 ; RRID:Addgene 12259).

A7R5 cells were induced towards the contractile phenotype using serum starvation, whereby plated cells previously grown in full (10% serum) were given either 0% serum, 2.5% serum, or the control 10% serum for 24 hours. [99]

Human aortic smooth muscle cells (HAoSMC) were obtained from ATCC (ATCC #PCS-100-012) and cultured using Vascular Cell Basal Media (ATCC, PCS-100-030) and the Vascular Smooth Muscle Cell Growth Kit (ATCC, PCS-100-042). All cells cultured and used in experiments were kept under P9. At 48 hours prior to each experiment, HAoSMC cells were transfected with 2 ug total DNA using the lipid based transfection system LipoD 293 DNA transfection reagent (SignaGen, catalog # SL100668).

FRAP

Fluorescence recovery after photobleaching (FRAP), was performed on A7R5 cells overexpressing EGFP-SM1A at 24 hrs post-transfection and on HAoSMC cells overexpressing EGFP-SM1A at 48 hours post transfection on a Zeiss LSM 880 Airyscan. Cells were imaged in Airyscan Fast mode at 1x Nyquist sampling for optimal confocal resolution at 1 Hz for up to 1200 seconds. A circular region (50 pixel diameter) was bleached using 405 nm, 458 nm, and 488 nm lasers at 100% laser power. For drug experiments, a cell was subject to FRAP, then carbachol or angiotensin ii was added, and then the same cell but unique bleach region was subject to FRAP again. Delay between drug addition and initiation of the second FRAP time-course was 30-60 seconds. FRAP analysis was performed in FIJI similar to previous protocols. [100] Three ROIs were measured for each experiment - a bleach region, a control region within

the cell, and a background region outside of the cell. Intensity was monitored over time in each region. Recovery within the bleach region was obtained after normalizing to the control region and subtracting the background region. Recovery curves were plotted in FIJI using the curve fitting plug in, fitting to a single exponential. The numbers given are used to calculate mobile fraction, t ½, and k_{off}.

Drugs Used and Concentrations

Table 2. Drugs Used and Concentrations

Drug	Company	Catalog Num	Concentration
Carbachol	Santa Crus Biotechnology	CAS 51 83 2	10 uM
Angiotensin II	Sigma Aldrich	CAS 4474 91 3	0.2 mM

Super Resolution Imaging of SM1A Filaments

Imaging of HAoSMC and A7R5 cells expressing EGFP-SM1A were collected on a Zeiss LSM 880 Airyscan. Imaged 48 hours and 24 hours post transfection respectively, Airyscan SR mode was used followed by Airyscan Processing.

SIM Imaging

A7R5 cells were transfected with EGFP-SM1A and mApple-NM2A. Images were collected on a Zeiss Elyra 7 Structured Illumination Microscope with a Plan-Apochromat 63x/1.4 NA oil DIC M27 objective. Scan Mode was FastFrame with 1.0 x zoom. Reconstruction was performed with SIM2.

Statistics

Statistics were performed using the GraphPad Prism. Specific tests used for each experiment are stated in figure legends. Asterisks are used to convey statistical significance are as follows: * for $p < 0.05$, ** for $p < 0.005$, *** for $p < 0.0005$.

Results

A7R5 Cells Express EGFP-SM1A and Correctly Localize the Fusion Protein

A single smooth muscle myosin gene (Myh11) with two splicing events produces four isoforms (SM1A, SM1B, SM2A, SM2B). [101] The dominant isoform in vascular SMCs is SM1A. [102,103] Therefore, to better understand the dynamics of smooth muscle myosin filaments in SMCs, we generated an expression plasmid with an EGFP coupled to the N-terminus of the SM1A heavy chain (hereafter EGFP-SM1A; Fig. 4). No construct labeling human smooth muscle myosin heavy chain existed previously, to my best knowledge.

After creation of this construct, we confirmed expression and localization by transfecting A7R5 cells and HAoSMCs. Western blot analysis of transient overexpression of EGFP-SM1A in A7R5 rat aortic SMCs demonstrated expression of the EGFP-SM1A shifted above endogenous smooth muscle myosin, as expected (Fig. 4 C). High resolution imaging demonstrated that EGFP-SM1A associated with large actin stress fibers in both the cell lines (Fig. 4 D), as expected from previous literature showing normal myosin filament assembly upon tagging the N-terminus of other class 2 myosins. EGFP-SM1A assembles correctly and localizes to filaments. Therefore, our EGFP-SM1A plasmid appears to be a faithful reporter of SM1A in these immortalized SMCs and in the human primary aortic smooth muscle cells.

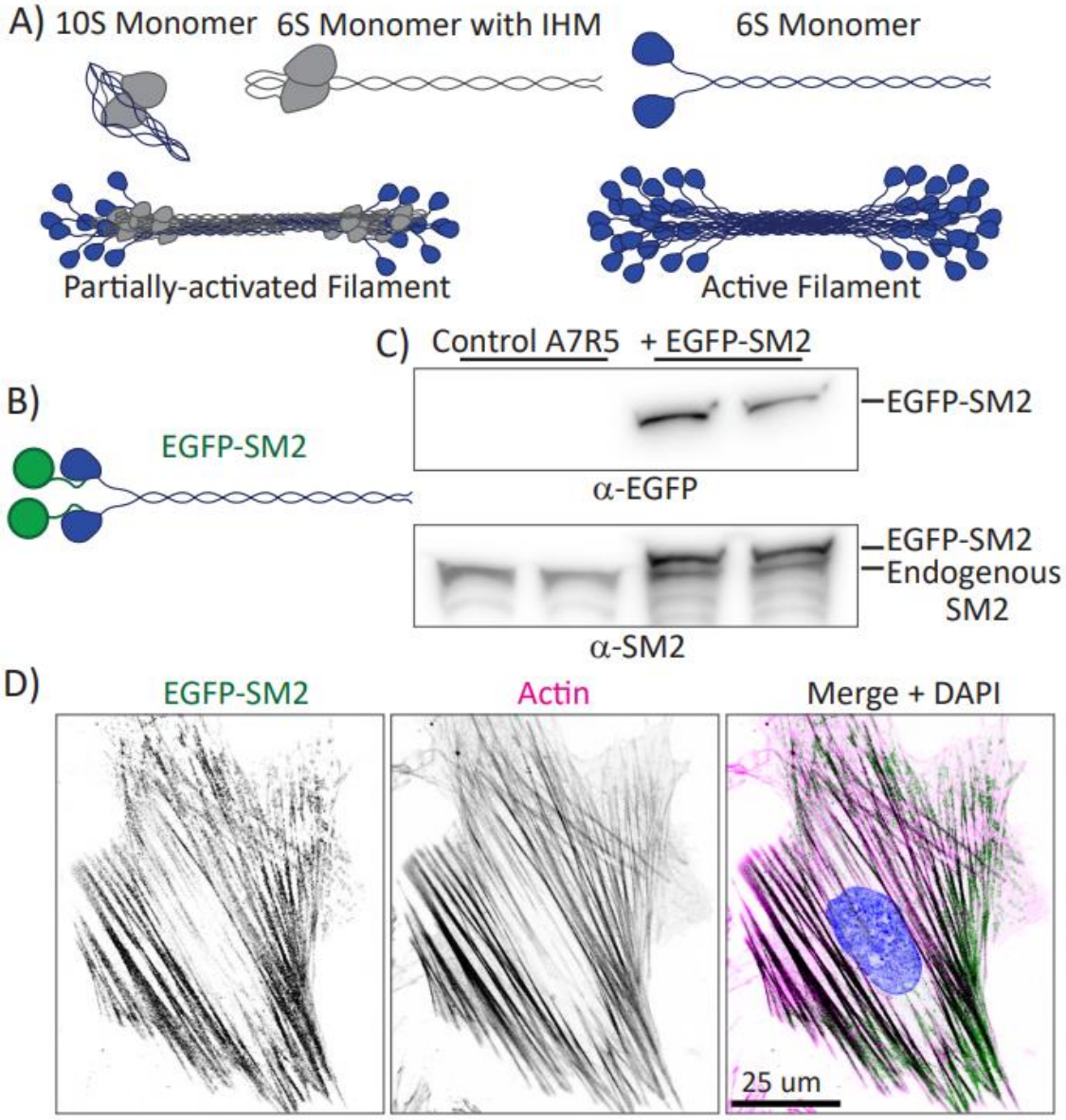

Figure 4. Expression of Endogenous SM1A and Fusion Protein EGFP-SM1A in A7R5 SMCs. A) Cartoon of myosin 2 monomeric and filamentous structural states. B) Cartoon of 6S SM1A monomer tagged on the N-terminus with EGFP. C) Western blot of A7R5 cells untransfected (left lanes; duplicate) or transiently expressing EGFP-SM1A (right lanes; duplicate) probed with a-EGFP (top blot) or a-MYH11 (bottom blot). D) Example images

of A7R5 cell transiently expressing EGFP-SM1A (green), fixed and stained with phalloidin (actin; magenta).

A7R5 Cells Expressing EGFP-SM1A Display Calcium and Contractile Response to Carbachol

As previously mentioned, the gold standard of smooth muscle studies would be to study smooth muscle myosin within the intact tissue; since that is not possible, it is important to validate that our cell line is an appropriate alternative. Specifically, we looked to ensure the A7R5 cell line produced a calcium and contractile response to drugs, thus allowing us to not only show that these cells are not fully undifferentiated, but also to characterize cellular response to drug activation. To confirm that our A7R5 cells are capable of induced contractility, we performed control experiments with the acetylcholine agonist carbachol. Carbachol increases cytoplasmic calcium concentration stimulating contraction in VSMCs.Carbachol treatment of GCaMP7s-expressing cells resulted in transient cytosolic calcium increases (Fig 5A & 5C). This confirms that A7R5 cells retain carbachol receptors and the ability to mount an appropriate calcium response. While A7R5 cells are not a perfect system, they retain many qualities of SMCs in tissue.

In parallel, we performed traction force microscopy (TFM) to confirm that these cytosolic calcium increases were harnessed into contractile energy. We observed contractile force generation following carbachol treatment with a slight delay and extended duration relative to the cytosolic calcium response (Fig. 5B and 5C), consistent with the calcium/MLCK-dependent signaling cascade that displays similar kinetics in intact smooth muscle tissue. [104] Together these results indicate that while A7R5 cells are not primary SMCs, they retain a

calcium-mediated contractile response to carbachol and can be used to investigate SM1A during induced activation.

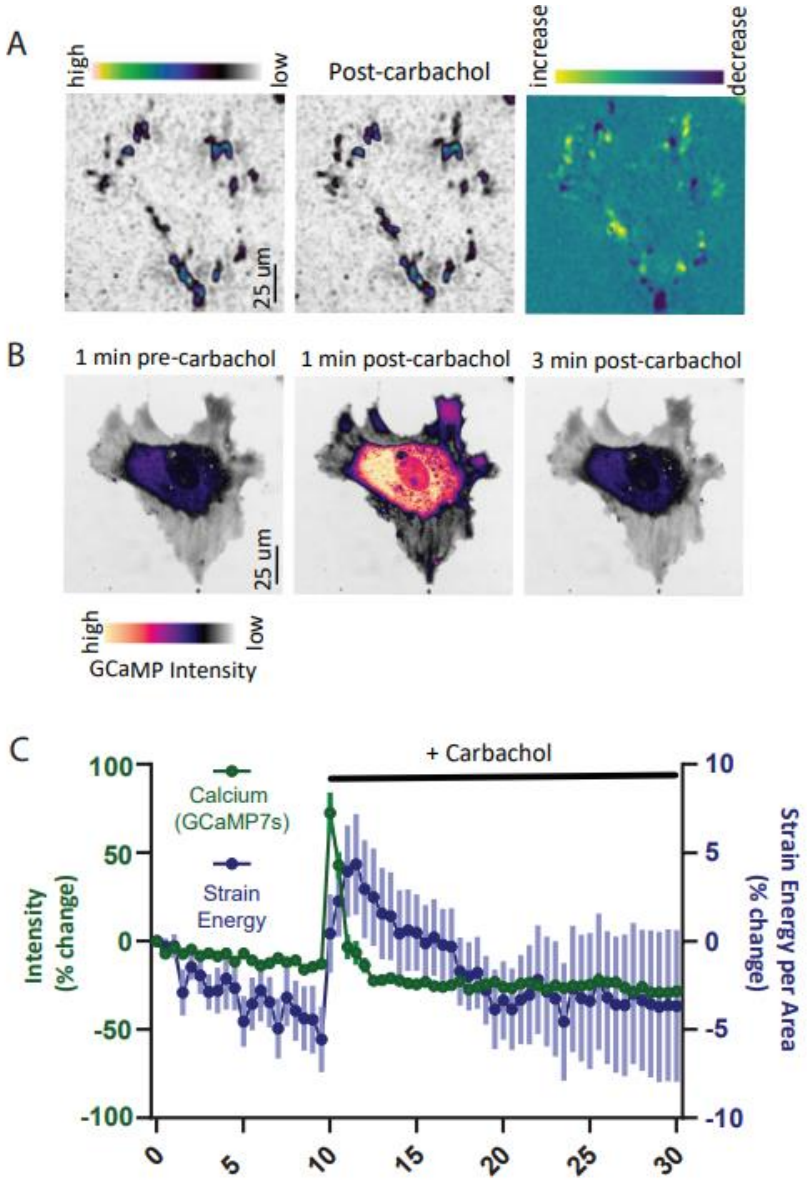

Figure 5. A7R5 Cells Show Measurable Calcium and Contractile Responses to Carbachol. A \& B) A7R5 cell expressing GCaMP7s was monitored for cytosolic calcium levels (A) while simultaneously being subject to traction force microscopy pre- and post-carbachol (B). GCaMP intensity and strain energy are displayed with iLUTs (scales on left). Pre-carbachol strain energy is the mean of 10 minutes pre-treatment and post-carbachol strain energy image is the mean of 10 minutes post-treatment. The delta between pre- and post-carbachol strain energy is displayed in the rightmost image. C) Quantitation of cytosolic

calcium (green) and strain energy per area (orange) over time. Data plotted as mean +/- SEM for 15 cells from 3 experiments.

SM1A Filaments are Highly Dynamic

The details of smooth muscle myosin dynamics have remained largely elusive for many years. We are specifically interested in the dynamics of a myosin monomer exchanging within a filament, rather than turnover of protein through synthesis and degradation (Figure 3.3). The filaments could be highly stable, and display a low amount of slow turnover, or could be highly dynamic displaying high rates of rapid turnover.

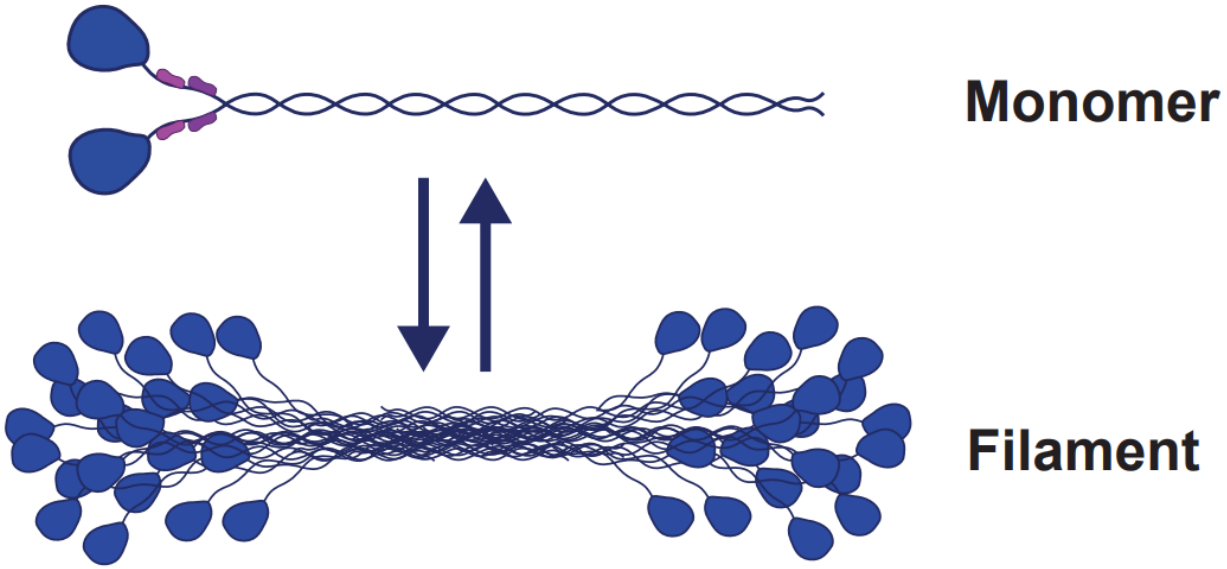

Figure 6. Model of Myosin Exchange Between Monomer and Filament. In speaking about "exchange" we are specifically discussing the movement of myosin monomers in and out of a filament. The larger structure of the filament can stay intact while monomers move in and out. It is this movement that we are measuring.

As mentioned before, smooth muscle myosin belongs to the larger class of myosins called the class 2 myosins. Among this class, the dynamics of each myosin varies greatly.

Skeletal muscle myosin is seen to exchange on the order of hours. [105] It has also been shown that the monomer pool within the myofibrils influences exchange rate. [106] Non-muscle myosin IIA has been shown to exchange on the order of 10s of seconds . [107] Taken together, this shows that class 2 myosins have a large range of dynamics, with skeletal muscle forming highly stable filaments and non-muscle myosin IIA forming highly dynamic filaments. Since smooth muscle myosin is related to both of these myosins, it is conceivable that the dynamics could mirror either skeletal muscle myosin or non-muscle myosin, or reside somewhere in between these two.

To investigate SM1A filament dynamics, fluorescence recovery after photobleaching (FRAP) was performed on A7R5 cells expressing EGFP-SM1A. Here, we use the term "exchange" to refer to the movement of myosin 2 monomers into and out of filaments, and avoid the term "turnover", which might also refer to protein synthesis and degradation, which should not be relevant during our experimental timescales (minutes). FRAP allows us to visualize and measure the amount of monomers exchanging within a smooth muscle myosin filament. Figure 7 shows an example of the quantitative data produced by this example along with how a smooth muscle myosin filament would appear. Before bleaching, fluorescence intensity is high and monomers within the filament are fluorescent. A high intensity laser irreversibly bleaches the fluorophores, turning that filament "dark". Because the bleaching is irreversible, the fluorescent signal recovery is due to new myosin monomers being incorporated into the filament. From this, we can measure mobile fraction, or how much myosin is exchanging and $t_{½}$, or how long it takes for half of the total recovery to occur. Finally, we can also measure k_{off}, or the rate in which bleached myosin monomers leave the bleach zone so new monomers can

come in. [108]

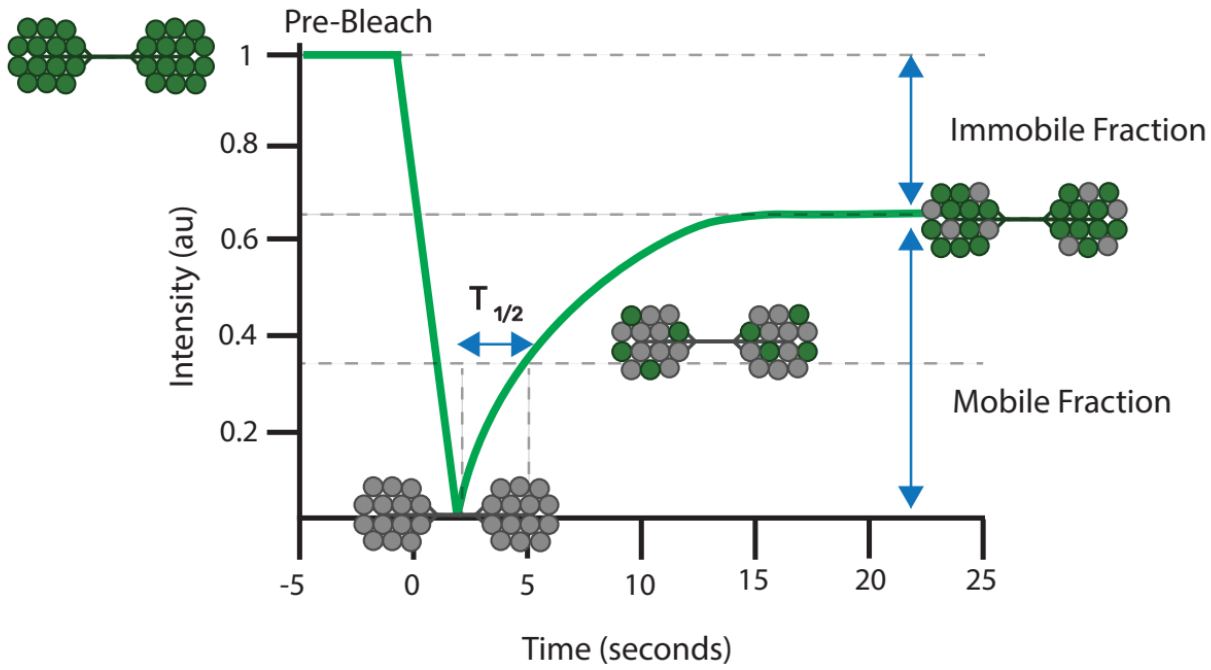

Figure 7. Description of FRAP Data Output. Fluorescent Recovery After Photobleaching, or FRAP, measures exchange by measuring how much fluorescence recovers in an area. First the cell is imaged to identify a baseline for fluorescence intensity. Then a region is bleached using a high intensity laser. Because the filament is bleached, any return in fluorescence is due to the exchange of new monomers into the filament. By measuring fluorescence recovery in that region we can measure how much of the filament is exchanging and how quickly that is happening.

Figure 7 shows an example EGFP-SM1A FRAP experiment, with insets showing SM1A before bleaching and during recovery. FRAP quantification includes the mobile fraction, which is the fraction of filamentous SM1A exchanging, and the t ½, which is the time it takes for half of the total exchange to occur. Our data reveal that SM1A filaments exchange readily (relatively high mobile fraction; Fig. 8B) and with rapid kinetics (relatively short t ½, Fig. 8C), relative to striated paralogs. [105] This is true in both the A7R5 cell line and the HAoSMC cell line,

indicating this is not a cell line specific phenomenon but rather an intrinsic property of smooth muscle myosin. This suggests SM1A forms highly dynamic filaments within SMCs that are more reminiscent of non-muscle myosin systems [83,84] than striated muscle myosin systems. [109] While class 2 myosins exchange on a wide spectrum of times, smooth muscle myosin falls on the side of more rapid turnover. This is not only important for comparison of smooth muscle myosin to other myosins, but also for understanding the fundamental nature of contraction within smooth muscle cells and how pathological mutations might alter dynamics.

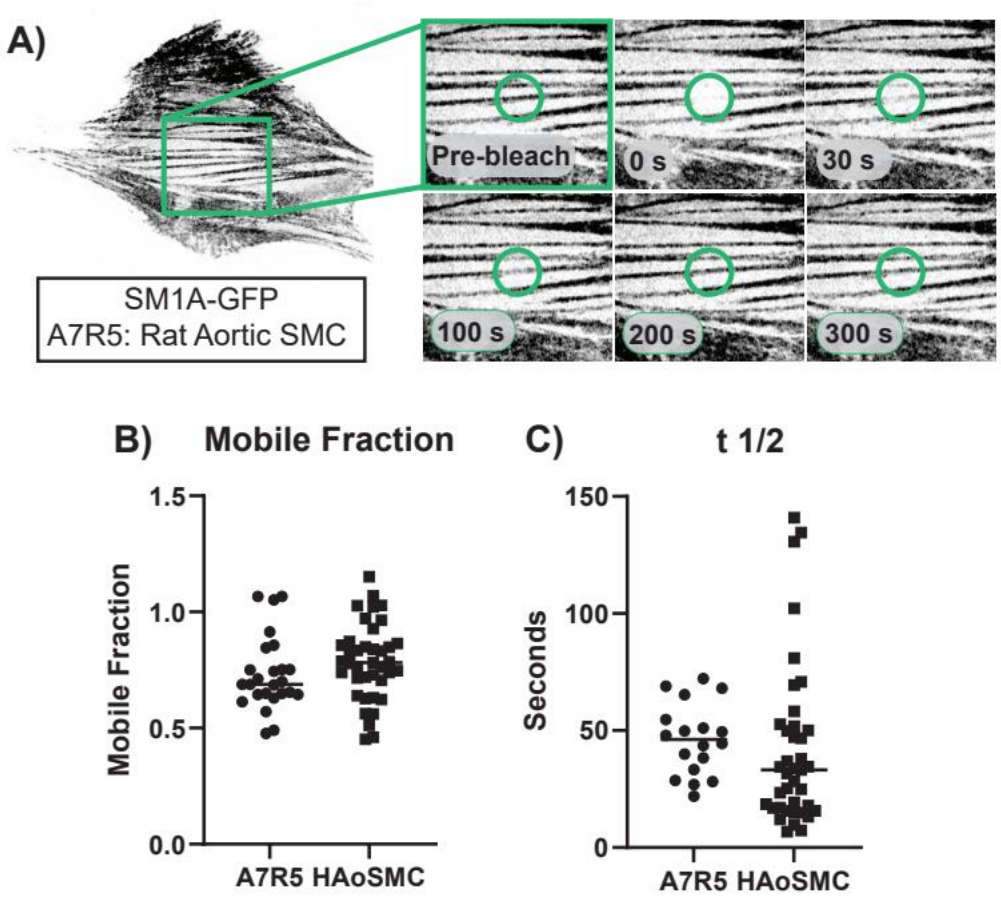

Figure 8. SM1A Filaments are Highly Dynamic. A) FRAP example A7R5 expressing EGFP-SM1A Bleach region indicated by green circle in insets. B & C) Mobile fraction (B) and t 1/2 (C) plotted for EGFP-SM2 expressing A7R5 cells and HAoSMCs from 3 independent experiments. Horizontal lines indicate mean.

Smooth Muscle and Non-Muscle Myosin Appear to Co-assemble

The kinetic and genetic similarity between SM1A and NM2, along with the fact that SMCs express both myosin 2 paralogs, led us to more carefully investigate their relationship in our cell model. Previous studies using structured illumination microscopy (SIM) to image coupled flurophores on the head or tail of NM2 isoforms have enabled filament identification and shown isoform co-assembly. [98] This approach reveals alternating head-tail-head patterns about 300 nm in length, indicative of individual filaments or small filament stacks.

We used a similar approach for SM1A and NM2 by co-expressing EGFP-SM1A and NM2A-mApple in A7R5 cells. SM1A and NM2A within the same filamentous structures would produce a green-magenta-green (head-tail-head) pattern (Fig. 9A). At the whole-cell scale, SM1A and NM2A were significantly co-localized along stress fibers (Fig. 9B). However, upon closer examination, we observed SM1A head domains about 300 nm apart flanking NM2A tails (Fig. 9C). While immuno-electron microscopy would more definitively confirm co-assembly in cells, our data suggest SM1A and NM2 isoforms can co-assemble in SMCs. [110]

This is a novel observation. It is also important to note that we have just observed that non-muscle myosin and smooth muscle myosin can co-assemble in cultured cells, not the extent at which they do in tissues. It has been shown that smooth muscle myosin isoforms may co-assemble with each other [67,75]; however, it has not been shown that smooth muscle myosin could assemble with other types of class 2 myosins. Non-muscle myosin has been shown to be instrumental in smooth muscle cell contraction. In fact, smooth muscle does have some level of contraction even in the absence of smooth muscle myosin. [36] [111] Non-muscle myosin may

be important for contraction maintenance in smooth muscle.[38] It is an interesting notion to think that some of this may be due to co-assembly of non-muscle myosin and smooth muscle myosin.

While our experiment includes non-muscle myosin throughout the cell, previous studies have shown non-muscle myosin to be localized towards the periphery of the cell. [40] Our experiment may not be a faithful reporter of where non-muscle localizes in tissues, but the point remains that our results indicate smooth and non-muscle myosins may co-assemble. In intact tissues, this could happen towards the periphery of the cell where non-muscle myosin has been seen.

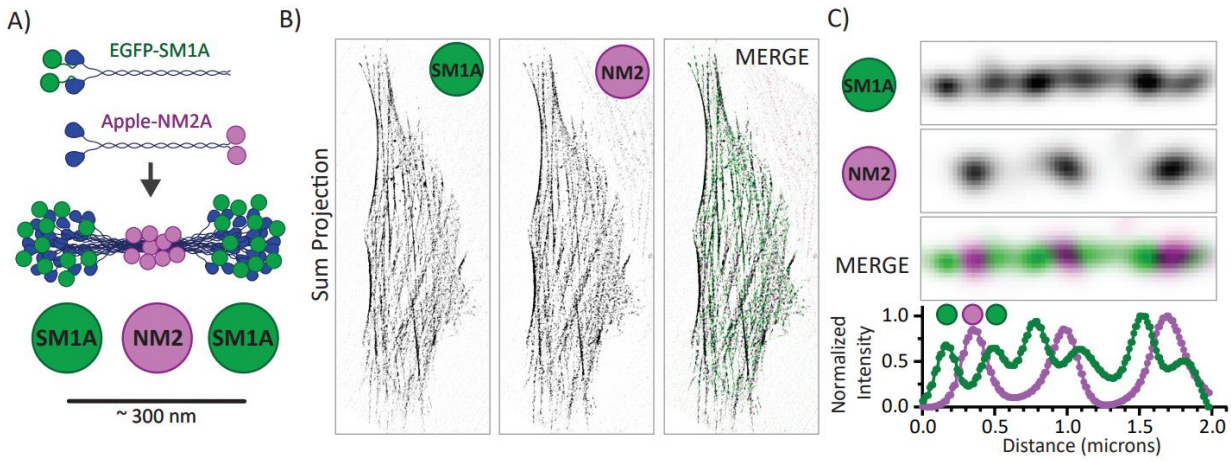

Figure 9. NM2 and SM1A Appear to Co-assemble. Cartoon of potential co-assembled filaments made up of EGFP-SM1A and NM2A-mApple. B) Co-transfection of EGFP-SM1Aand NM2A-mApple in A7R5 cells were imaged with SIM and sum projected. Individual channels are displayed in inverted greyscale and merge is shown in the right panel. C) An individual actomyosin fiber was cropped from the cell in (B) and displayed at higher zoom for SM1A , NM2 and merge. The lower plot is a line scan through the fiber normalized to maximum intensity for each channel.

To further investigate the possibility of co-assembly between smooth muscle myosin and non-muscle myosin immuno-electron microscopy could be used. EM images of filaments with non-muscle myosin and smooth muscle myosin deferentially labelled would allow confirmation of co-assembly. This would allow for not only confirmation of assembly, but would also provide better insight in how much of the filaments are co-assembled heterofilaments. My data suggests the two myosins are highly co-assembled, with near complete overlap in the EGFP-SM1A and NM2A-mApple channels, and this could be confirmed by EM.

Dynamics Between Smooth Muscle Myosin and Non-Muscle Myosin are Nearly Identical

Because of similarities between smooth muscle myosin and non-muscle myosin 2A, and the imaging suggesting co-assembly, we decided to investigate dynamics of both within SMCs. To better quantify the similarity in dynamics of SM1A and NM2, we performed simultaneous FRAP in the dual-expressing cells. By eye, there is no visible difference in fluorescent recovery (Fig. 10A). This is confirmed by the recovery curves; recovery curves for both proteins (Fig 310C) display nearly identical recovery. Quantification shows indistinguishable mobile fractions (Fig 10D) and t ½ (Fig 10E) indicating that both SM1A and NM2A filaments turnover rapidly and readily in SMCs. Collectively then, SM1A filaments in cultured SMCs co-localize with NM2 in filamentous structures that suggest co-assembly, and display rapid polymer exchange kinetics that are indistinguishable from NM2.

Differentiation to a "Contractile" Phenotype Does not Alter Filament Dynamics

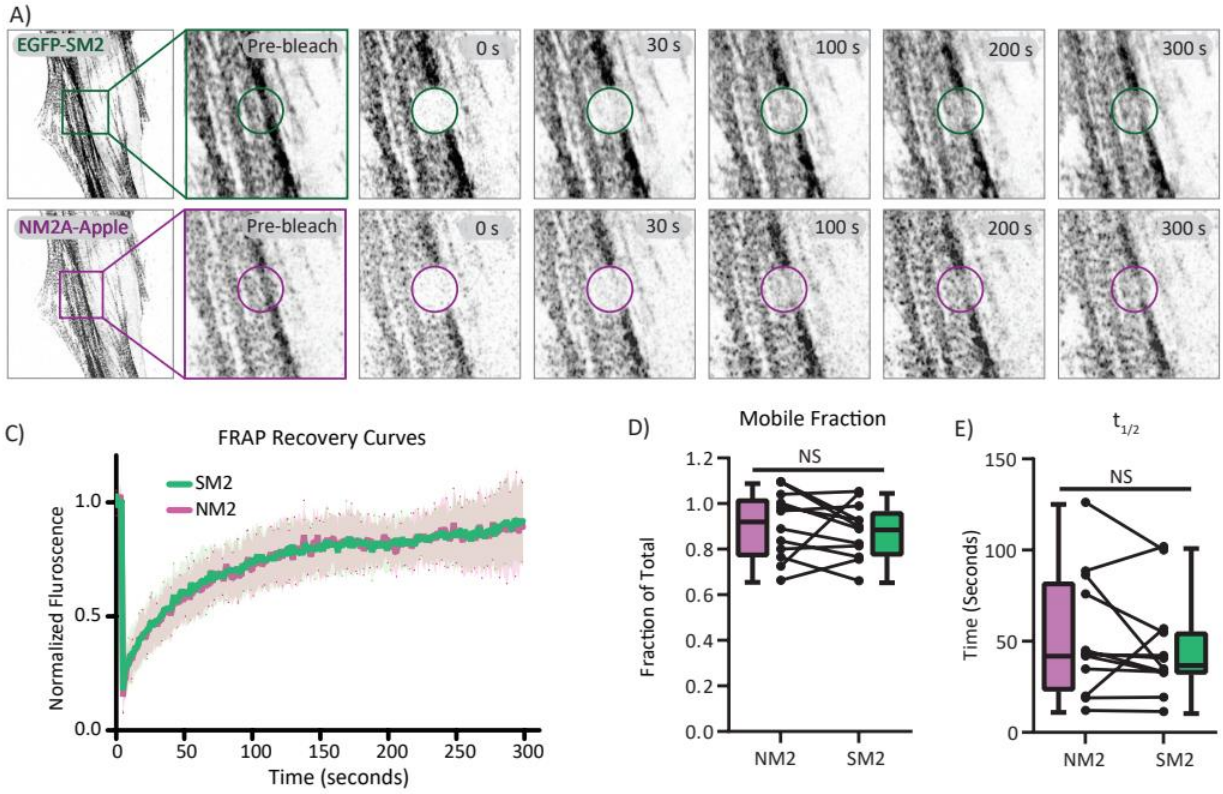

Figure 10. SM1A Filaments are Highly Dynamic and Similar to NM2. A) FRAP example of A7R5 expressing EGFP-SM1A (top row) and NM2A-mApple (bottom row). Bleach regions indicated by circles. C) Recovery curves of SM1A and NM2 plotted as mean +/- SEM for 12 cells from 3 independent experiments. D \& E) Mobile fraction (D) and t1/2 (E) displayed as both box and whiskers (median +/- quartiles) and spaghetti plot. Dots in spaghetti plot represent individual cells for NM2 and SM1A with lines connecting cells. A paired t-tests was performed and there was no statistically significant difference between groups.

As mentioned previously, SMCs can exist along a continuum between two phenotypes - contractile and synthetic. The contractile phenotype is found in healthy contracting blood vessels while the synthetic phenotype is more proliferative and migratory and is associated with

pathological states (e.g. atherosclerosis). [99]

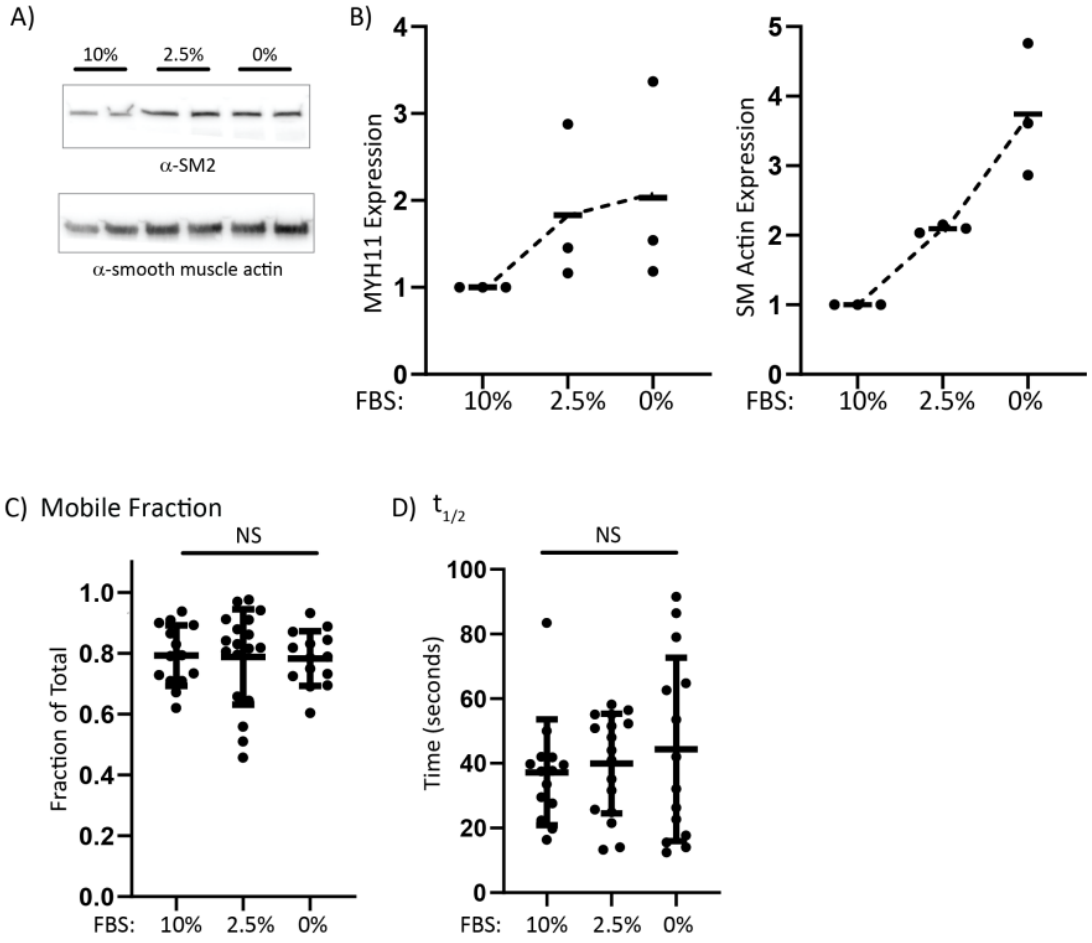

Figure 11. Differentiation to a More Contractile Phenotype does not Change Filament Dynamics. A & B) A7R5 cells cultured in media with 10%, 2.5%, or 0% FBS in duplicate were subject to western blot analysis with a-MYH11(top blot) and a-smooth muscle actin (bottom blot). Cumulative data plotted in B as mean +/- SD from 6 samples per condition from 3 independent experiments. C \& D) FRAP was performed on A7R5 cells expressing EGFP-SM2 cultured in media containing the indicated levels of FBS. Mobile fraction and t ½ plotted as the mean of 14-18 cells per condition over 3 individual experiments. One way ANOVA performed between groups and showed no difference.

We wanted to determine if SM1A assembly dynamics were altered upon induction of a prolonged contractile phenotype using serum starvation of A7R5. [97]

To confirm differentiation of the A7R5 cells following serum starvation, expression of contractile proteins was measured by western blot. Expression of contractile proteins in cells experiencing various serum conditions shows that serum starvation increases both smooth muscle and smooth muscle actin, confirming the protocol has pushed the cells towards a contractile phenotype (Fig 11A & 11B). However, FRAP analysis revealed that SM1A polymer exchange kinetics were unaltered, as there was no difference in mobile fraction or t½ between serum starved or non serum starved cells (Fig. 11C and 11D). In a more synthetic phenotype or in a more contractile phenotype, smooth muscle myosin exchange is unaltered. This suggests that dynamics are conserved across SMC phenotypes, or that our experimental model only explores a relatively narrow portion of the contractile-synthetic SMC continuum.

SM1A Filament Dynamics are Modulated Upon Transiently-induced Contraction

To examine the impact of transiently inducing contraction in SMCs to mimic physiological activation, we performed FRAP before and after the addition of carbachol, a cholinergic agonist which stimulates release of intracellular calcium via IP3. [112] To closely observe relative changes in polymer exchange kinetics, we performed FRAP on a small region of an A7R5 expressing EGFP-SM1A, then treated with carbachol, and immediately performed FRAP on a similar but distinct region of the same cell (Fig. 12A and 12B). This provided cell-specific internal controls to monitor relative changes in assembly dynamics. We observed an increase in mobile fraction (Fig. 12D), suggesting more complete filament exchange, but also an

increase in t ½ (Fig. 12E), normally indicative of reduced exchange kinetics. However, because an increased mobile fraction with the same exchange kinetics would also lead to an increase in t ½, we analyzed the k_{off} parameter in the exponential recovery equation, a more comparable exchange rate indicator. Indeed, we observed that k_{off} was reduced upon treatment with carbachol (Fig. 12F), indicating reduced exchange kinetics and network stabilization.

We repeated this experiment in the HAoSMCs to assess if this effect was cell line specific. We used angiotensin II which has been known for decades to be a strong regulator of vascular tone. [113] By binding to the AT1 receptor, and working through IP3, angiotensin II can increase intracellular calcium within seconds. [114] We performed FRAP on a small region of HAoSMCs overexpressing EGFP-SM1A by bleaching a region and measuring recovery before adding angiotensin II and bleaching the same cell again in a different region and measuring recovery. In the HAoSMCs we saw a modest, but not statistically significant increase in mobile fraction. In contrast, we did see a statistically significant difference in the mobile fraction of EGFP-SM1A in A7R5 cells treated with carbachol, albeit modest. In the HAoSMC cells, we saw an increase in t ½, and reduction in k_{off} (Fig. 12 D & E). While the mobile fraction changes are not identical, the increase in t ½, and reduction in k_{off} in both cell lines indicate that the overall trend is consistent, making the conclusion more robust. Taken together, this shows SM1A filaments are stabilized during induced contractility in human primary aortic smooth muscle cells. This similar data in both cell lines confirms this is neither cell specific nor drug specific.

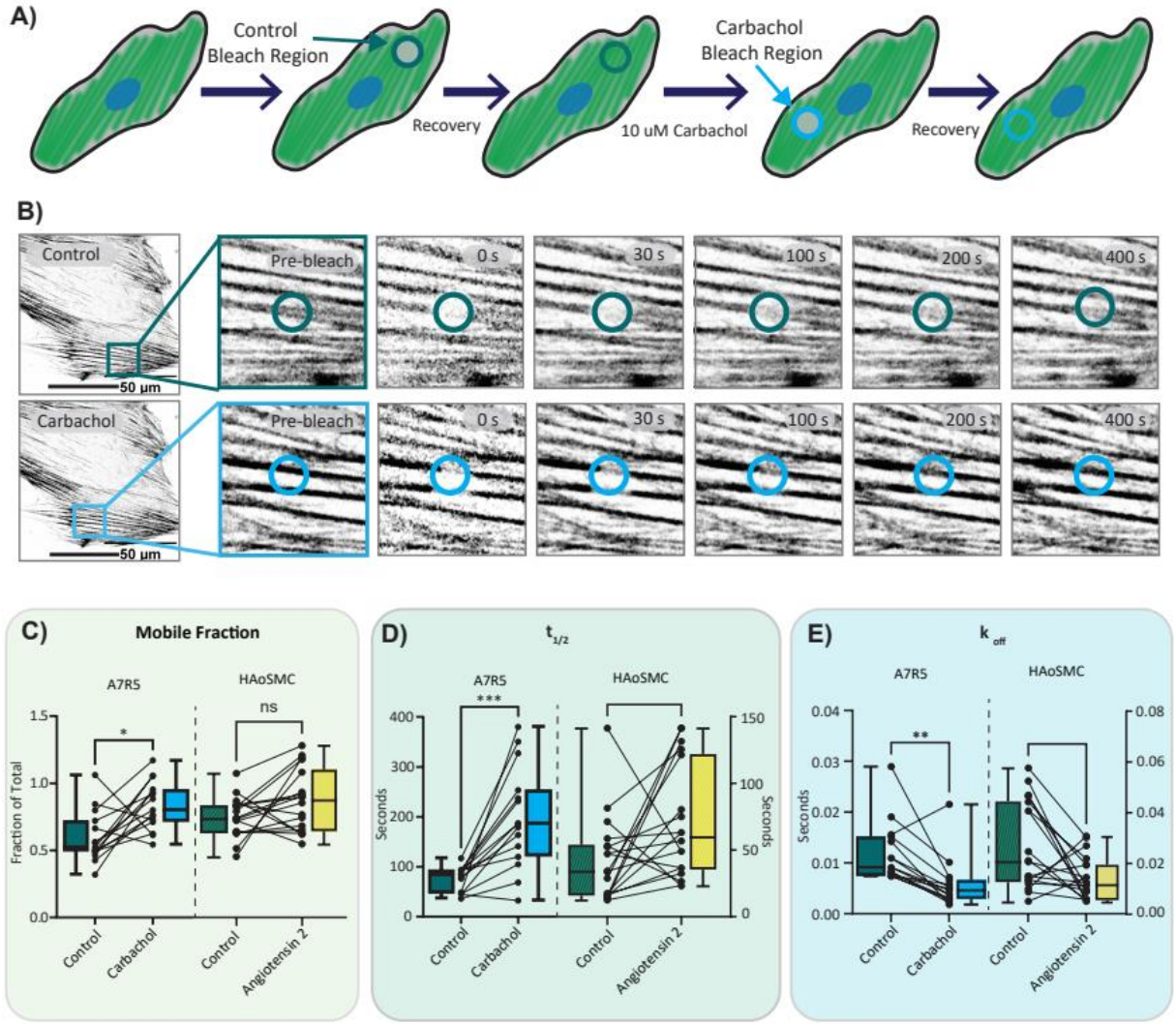

Figure 12. SM1A Filament Dynamics are Modulated Upon Induced Contraction. A) Schematic of experimental design for FRAP of a single cell before and after addition of 10 uM carbachol. B) Fluorescence recovery of EGFP-SM1A in A7R5 pre- (green) and post (blue) carbachol. Circles indicate bleach region. C) Mobile fraction (D) t1/2 (E) k_{off} of cells from 3 independent experiments. Cells are represented as dots in a spaghetti plot where pre- and post-drug measurements for individual cells are connected. The same data is also displayed as box and whiskers (median +/- quartiles). Paired t-tests were formed between control and carbachol/angiotensin II cells when measuring mobile fraction, t ½, and k_{off}.

Summary and Discussion

Our work indicates that smooth muscle filaments are dynamic (1), these dynamics are modulated as filaments are stabilized during induced contractility (2), and smooth muscle dynamics nearly identically mimic those of NM2.

Smooth muscle myosin forms highly dynamic filaments, especially when compared to other myosins like skeletal muscle myosin. This may not be surprising, as the overall stability of the contractile units in skeletal muscle and smooth muscle are vastly different. Although the range of exchange between smooth muscle and skeletal muscle is profound.

This rapid exchange may help smooth muscle cells to contract at a variety of different lengths, and to a fraction of their original size. Both of these are features that make smooth muscle unique from other muscle types, and swift exchange of smooth muscle myosin within filaments may contribute. Filaments need be assembled and modulated at a rapid rate to respond to changing conditions, and highly dynamic filaments are better at the quick evolution needed.

Different smooth muscle cell types have different contractile needs. For instance, vascular smooth muscle cells in smaller muscular arteries contract the blood vessel down to nearly eliminate the lumen. Bladder smooth muscle cells expand and then contract to a fraction of the original size. While other smooth muscle cells, like ciliary body smooth muscle cells in the eye, are required to produce a smaller degree of contraction. It is plausible that as rapid dynamics may be important in producing force at a variety of lengths, these dynamics may be altered in various tissues and isoforms in accordance to their needs.

Not only do filaments have rapid exchange, but this exchange can be modulated. My data demonstrates filament stabilization during induced contractility. This could be occurring as active motor heads interacting with actin are blocking monomer exchange from occurring. However, the consequences of this process being impeded is unclear. What changes in contractility may occur if filaments are not stabilized during activation? Or conversely, if exchange occurs more rapidly? The functional consequences of these questions remain unknown, but provide interesting fodder for future experiments.

Finally, we also saw that smooth muscle myosin dynamics mirror that of NM2, and these two myosin may even co-assembly. While preliminary data, and limited by our lack of visualization in tissue, this is an interesting find. We see that smooth muscle myosin and non-muscle myosin appear to be able to assemble, but to what extent that happens in tissues has yet to be determined. Smooth muscle is a broad classification and between tissues it has a wide variety of behaviors. Co-assembly of NM2 and smooth muscle myosin, and different amounts of heterofilaments, may be contributing to this large variation in contractile behaviors.

CHAPTER 4

SMOOTH MUSCLE MYOSIN FILAMENT ASSEMBLY

Materials and Methods

Cell Culture and Transfection

Rat aortic smooth muscle cell line, A7R5 cells, were obtained from ATCC and cultured in DMEM (MT10013CV, Corning) supplemented with 10% fetal bovine serum (MT35-010-CV, Corning) and 1% antibiotic–antimycotic solution (MT30004CI, Corning). At 24 hours prior to each experiment, A7R5 cells were transfected with 2 ug total DNA using the lipid based transfection system LipoD 293 DNA transfection reagent (SignaGen, catalog \# SL100668).

A7R5 cells were induced towards the contractile phenotype using serum starvation, whereby plated cells previously grown in full (10% serum) were given either 0% serum, 2.5% serum, or the control 10% serum for 24 hours. [99]

Human aortic smooth muscle cells (HAoSMC) were obtained from ATCC (ATCC #PCS-100-012) and cultured using Vascular Cell Basal Media (ATCC, PCS-100-030) and the Vascular Smooth Muscle Cell Growth Kit (ATCC, PCS-100-042). All cells cultured and used in experiments were kept under P9. At 48 hours prior to each experiment, HAoSMC cells were transfected with 2 ug total DNA using the lipid based transfection system LipoD 293 DNA transfection reagent (SignaGen, catalog # SL100668).

Single Cell Assembly Assay

The single cell assembly assay was performed on A7R5 cells transiently overexpressing

EGFP-SM1A. Cells were plated in a 96 well coverglass bottom dish (#655891, Greiner). Total EGFP-SM1A signal was collected for 16 positions per well. If applicable, small molecules were added and cells incubated for the indicated time. Then, triton buffer (5 uM PEG800, 100 mM PIPES, 150 mM NaCl, 1 mM EGTA, 1 mM MgCl2, 0.5% triton, 90% H20) was added to permeabilize the cells and release soluble EGFP-SM1A. The exact same positions were re-imaged to collect the triton-insoluble EGFP-SM1A signal. Individual cell masks were manually identified using FIJI. Local background fluorescence and mean fluorescence intensity was measured for each cell before and after permeabilization. Fraction assembled was then calculated as background subtracted signal post-permeabilization relative to background subtracted signal pre-permeabilization.

Results

Induced SMC Contraction Enhances SM1A Filament Assembly

Filament assembly in response to contractile stimuli has been studied previously. Smolensky et al found that smooth muscle myosin filaments increased in thickness in response to stimuli, and by inhibiting RLC phosphorylation, this phenomenon is ameliorated. [77,115] Using birefringence and EM, they found that the diameter of filaments increased during contraction. This suggests that filaments are assembled or reinforced or thickened during contraction. However, this does seem to be possibly due to filaments thickening as contraction occurs, but the same amount of total myosin assembled remaining constant. It is unknown what fraction of smooth muscle myosin is in filaments at these time points. A monomer pool has been observed in tissues, with the self inhibited form of smooth muscle myosin monomers present in the cytoplasm.[47] But the function, role, and dynamic size of the monomer pool is yet to be

discerned. So while it has been seen that myosin assembly increased after activation, what fraction of myosin is in the monomeric vs filamentous pools over time is unknown. Using a new imaging based assembly assay, we were able to confirm filament assembly upon activation and add depth to this story. We were not only able to measure change in total filaments but also in the monomer pool informing how much of total myosin is used in filaments at steady state and during induced contractility.

To investigate SM1A assembly, we performed a single-cell imaging-based triton permeabilization assay to measure populations of monomeric and filamentous myosin on two cell lines - A7R5 and HAoSMC - both expressing EGFP-SM1A. This assembly compares amounts of total myosin and filamentous myosin by measuring mean fluorescence intensity before and after permeabilization and washing away of smooth muscle myosin monomers. A7R5 cells expressing EGFP-SM1A were imaged to measure total EGFP-SM1A intensity, treated with or without carbachol, permeabilized with a triton buffer to remove monomeric SM1A pool, and re-imaged to measure remaining filamentous signal (Fig. 13A & 13B). Comparing intensity differences pre- and post-triton enables quantitative determination of monomer/filament ratios on a single cell basis. Control experiments with A7R5 cells expressing a diffuse EGFP reveal a complete loss of EGFP signal upon triton permeabilization, demonstrating cytosolic proteins are completely liberated in this assay (Fig. 13C).

Control assembly levels for SM1A were ~75% filamentous in the A7R5 cell line and approximately ~60% filamentous in the HAoSMC cell line (Fig. 13D and Fig. 13E). We don't have a clear explanation why smooth muscle myosin is less assembled in the primary cell line. It may be that HAoSMCs exist at a more relaxed state in culture than A7R5 cells and therefore are

less assembled. In the A7R5 cell line we observed no difference in this steady-state assembled fraction upon serum starvation (Fig. 13E). Serum starvation induces differentiation and increases the total amount of contractile proteins. However, an increase in smooth myosin expression does not appear to alter the fraction of myosin assembled.

To examine how filament assembly may be altered upon induced contraction, we repeated the single cell assembly assay with the addition an agonist to activate the cells and induce contractility. In the A7R5 cell line we used carbachol to induce contraction and in the HAoSMC cell line we used Angiotensin ii. Both are commonly used activators of smooth muscle cells. Within one minute of carbachol addition to the A7R5 cell line, assembly levels increased ~10% before decreasing towards steady-state levels in the ensuing minutes (Fig. 13D). Notably, these assembly kinetics parallel the cytosolic calcium response and traction force measurements during induced contractility (Fig. 11). A similar trend was present in the HAoSMC expressing EGFP-SM1A treated with angiotensin ii, where we observed a slightly delayed response but greater overall assembly response relative to the A7R5. While kinetics vary, both cell lines show a marked increase in filamentous myosin upon induced contractility.

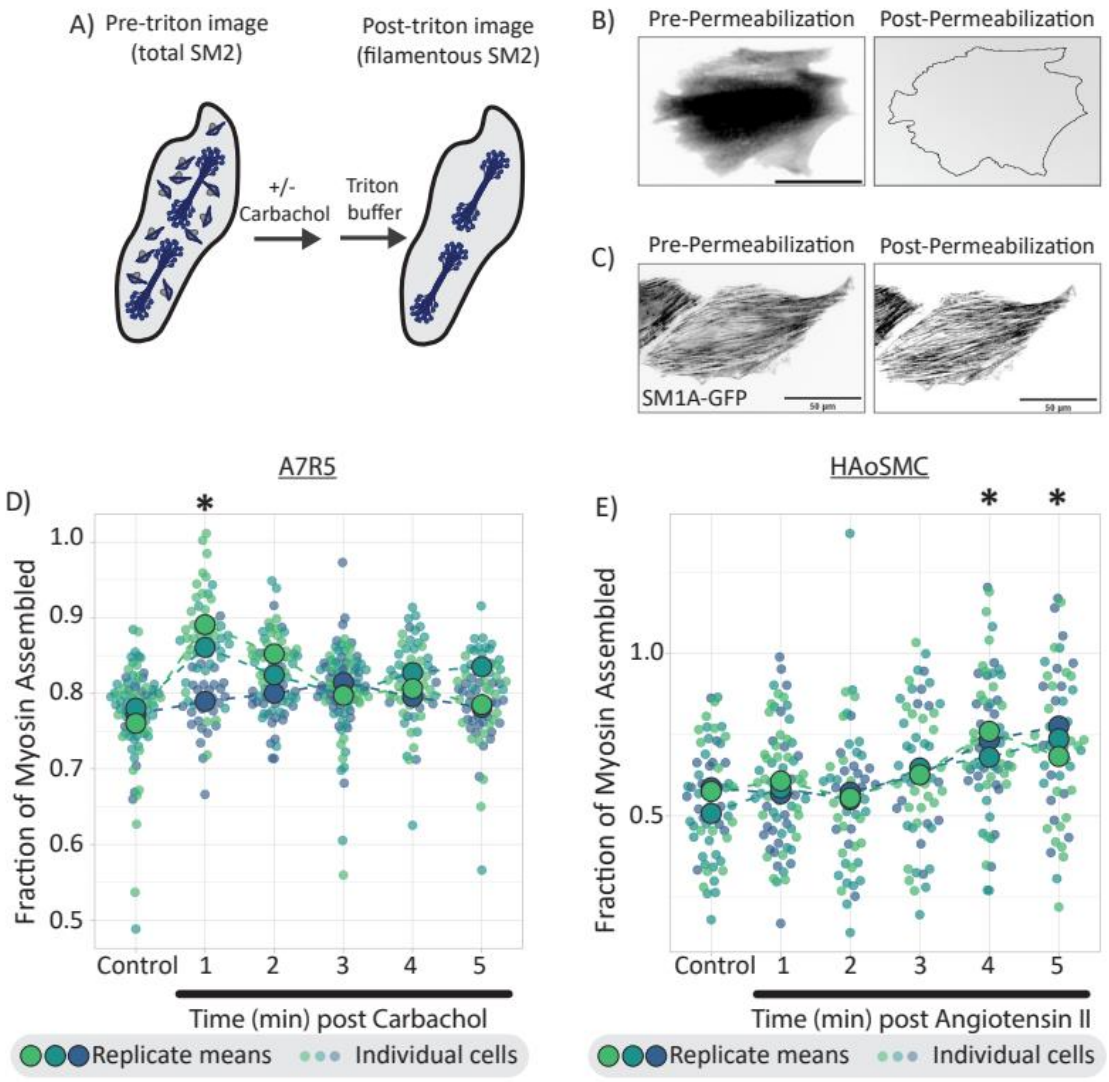

Figure 13. Induced Contraction of SMCs Induces SM2 Assembly. A) Cartoon illustrating single-cell assembly assay. Live A7R5 cells expressing EGFP-SM2 were imaged to determine total SM2 intensity (left). Cells were treated with or without 10 uM carbachol for the indicated time, monomeric SM2 was extracted using a triton buffer, and a second image was taken to determine the intensity of the remaining filamentous SM2. (B) Proof of concept A7R5 cells expressing EGFP were imaged pre- and post-permeabilization to demonstrate cytoplasmic proteins are fully extracted from the cell. C) Example image of EGFP-SM2 expressing A7R5 cell pre- and post-permeabilization. D) Quantification of the fraction of SM2 assembled in control cells and cells treated with 10 uM of carbachol for the indicated time. Small circles indicate individual cells. Larger dark circles indicate means of three independent experiments. Paired t-tests were performed comparing each group to the control. A one-way Anova was used with multiple comparisons between each time point and control to statistically analyze the data.

Therefore, in addition to stabilization and activation of SM1A filaments, induced

contraction results in nascent filament assembly.

To confirm that the fraction of myosin assembled is not a direct result of overexpression, we plotted mean fluorescence intensity before permeabilization against fraction of myosin assembled in A7R5 cells expressing EGFP-SM1A at steady state (Fig 14). If overexpression were to change myosin assembly patterns, then it would be expected there would be a positive linear relationship between mean fluorescence intensity and fraction assembled. However, this is not the case. Therefore overexpression of EGFP-SM1A is not meaningfully altering a fraction of smooth muscle myosin assembled. This is consistent with the assembly data collected from differentiated A7R5 cells, where serum-starvation and subsequent increase in myosin expression did not result in higher myosin assembly levels (Fig 15).

Together this demonstrates smooth muscle myosin assembly levels are regulated independent of total amount of myosin present.

Summary and Discussion

Not only is each smooth muscle myosin filament dynamic, but the network of filaments is dynamic as well. Our data supports previous data by Smolensky et al which showed a similar phenomena. [77] While it has been shown that a monomer pool exists, and that filamentous myosin increases upon activation, the quanitative relationship between these two remained unknown. [47] Through our work we were able to quantitatively demonstrate that the monomer pool decreases, and filament assembly increases upon induced contractility. Furthermore, we could quantify how much of the total myosin is in the filamentous state versus monomeric throughout this process.

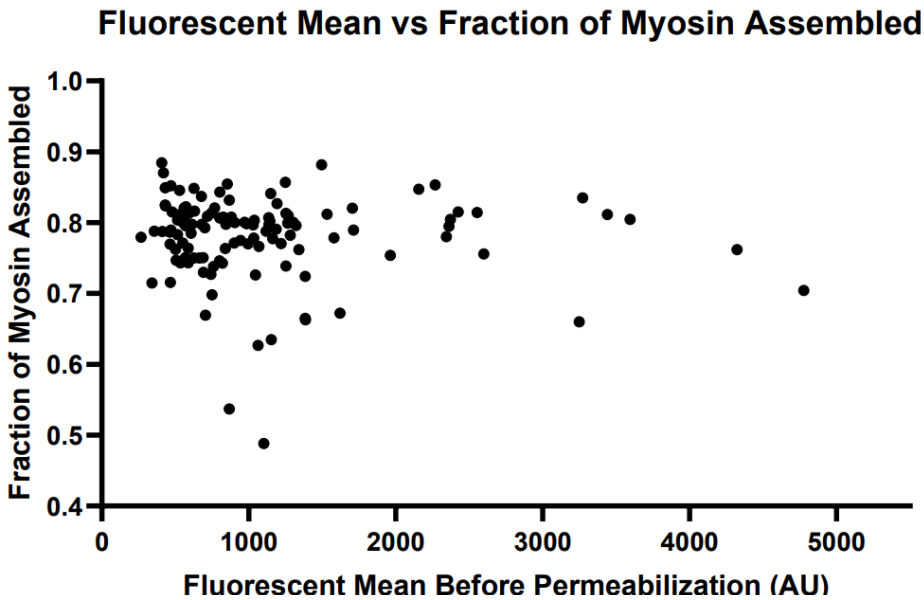

Figure 14. Fluorescent Mean vs Fraction of Myosin Assembled. Each dot represents a single cell from three separate experiments.

In this sense, our work has added to the depth of knowledge in the field, while also providing benchmarks to measure against, especially when analyzing pathological mutations that might alter assembly levels. However, it is also important to note some limitations of this study, and limitations in applying this conclusion broadly. We are specifically studying the SM1A isoform of smooth muscle myosin.

This means that the exact fraction of myosin assembled may be different in other isoforms, or in other tissues. We are limited in the study by the isoform used, the cell line used, and the caveat that this is in cell culture. Further experiments to carefully dissect the assembly of each isoform in physiological conditions would be ideal.

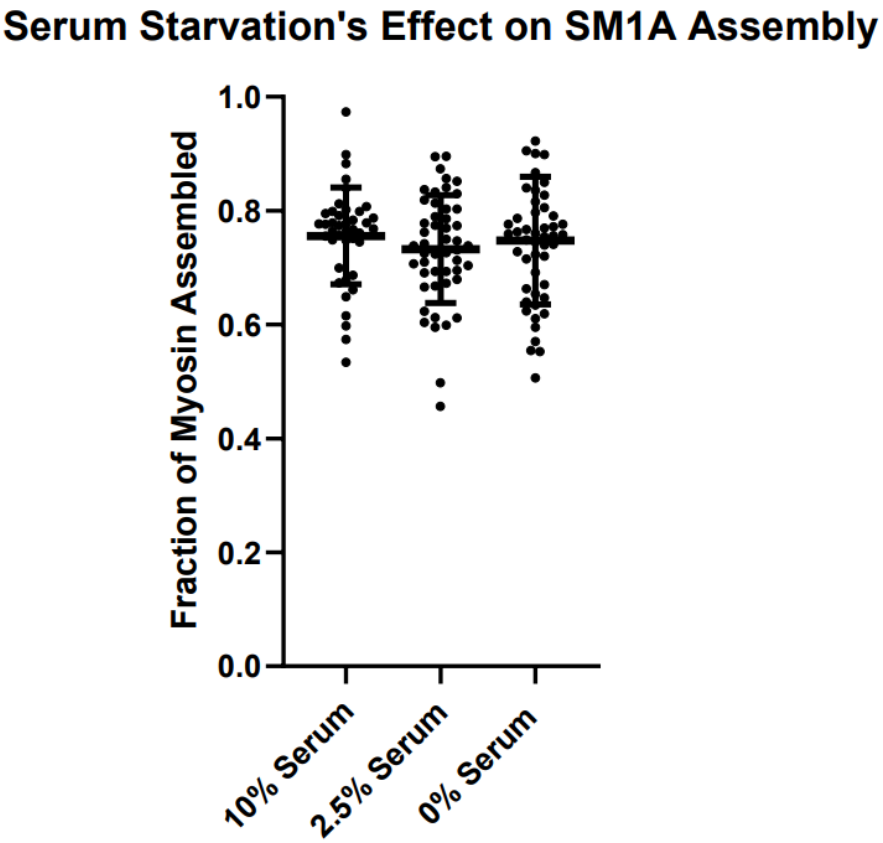

Figure 15. Differentiation Does not Alter Filament Assembly. Fraction of myosin assembled is measure for A7R5 cells overexpressing EGFP-SM1A cultured in 10\% serum, 2.5\% serum, and 0\% serum. Each circle represents a single cell. Mean and SD are plotted as lines. Data from three separate experiments is shown. One way anova was performed to determine if there was a statistically significant difference between groups. None was found.

However, with these limitations in mind, my data provides foundational insight into filament assembly, and while the exact fractions of smooth muscle myosin assembled may vary in different experiments, the mechanistic insight provided here sets a benchmark for others to build on.

CHAPTER 5

THE EFFECT OF PATHOLOGICAL MUTATIONS OF SMOOTH MUSCLE MYOSIN FILAMENT ASSEMBLY AND DYNAMICS

Materials and Methods

Mammalian Expression Vectors

To make each mutant construct, gBlocks were purchased containing the p.R1275L and p.A1839V mutations and then ligated into the previously made pEGFP-SM1A creating a pEGFP-SM1A-R1275L and pEGFP-SM1A-A1839V. By fluorescently labeling each of these mutated myosins we can measure how mutations affect smooth muscle myosin dynamics.

Cell Culture and Transfection

Rat aortic smooth muscle cell line, A7R5 cells, were obtained from ATCC and cultured in DMEM (MT10013CV, Corning) supplemented with 10% fetal bovine serum (MT35-010-CV, Corning) and 1% antibiotic–antimycotic solution (MT30004CI, Corning). At 24 hours prior to each experiment, A7R5 or JR20 NM2A knockout cells were transfected with 2 ug total DNA using the lipid based transfection system LipoD 293 DNA transfection reagent (SignaGen, catalog # SL100668).

Additionally a fibroblast cell with non-muscle myosin 2A knocked out was used. The line was produced by Hiral Patel in the Beach Lab using the following protocol:

Generation of KO Cells

HEK293T cells were transfected with LV-gRNAs and media containing virus was

harvested 48hour and 72 hour post transfection. JR20s (fibroblast cell line) were transduced with media containing virus collected 48 hours after transfection. The following day, JR20 cells were again transduced with virus containing media. Cells were then placed in antibiotic resistance using puromycin and hygromycin.

Validation of KO Cells

Confirmation of non-muscle myosin 2A KO was done using western blot. Lysates were collected and after running on an SDS-PAGE, proteins were transferred to a PVDF membrane. The membrane was blocked with 5% BSA for 60 min and incubated with the antibody against NMIIA (ECM biosciences) for overnight at 4C. Next day, after washing, the membrane was incubated with a anti Rabbit secondary antibody for 60 min.

The use of this cell line allowed us to examine filament formation in the absence of any complicating factors, such as endogenous WT smooth muscle myosin, filament stabilizing proteins, etc.

FRAP

Fluorescence recovery after photobleaching (FRAP), was performed on A7R5 cells overexpressing EGFP-SM1A-A1839V or EGFP-SM1A-R1275L at 24 hrs post-transfection on a Zeiss LSM 880 Airyscan as previously described. Cells were imaged in Airyscan Fast mode at 1x Nyquist sampling for optimal confocal resolution at 1 Hz for up to 1200 seconds. A circular region (50 pixel diameter) was bleached using 405 nm, 458 nm, and 488 nm lasers at 100\% laser power. FRAP analysis was performed in FIJI similar to previous protocols. [100] Three ROIs were measured for each experiment - a bleach region, a control region within the cell, and a background region outside of the cell. Intensity was monitored over time in each region.

Recovery within the bleach region was obtained after normalizing to the control region and subtracting the background region. Recovery curves were plotted in FIJI using the curve fitting plug in, fitting to a single exponential. The numbers given are used to calculate mobile fraction, t ½, and k_{off}.

Single Cell Assembly Assay

The single cell assembly assay was performed on JR20 NM2A KO cells transiently overexpressing EGFP-SM1A mutants. Cells were plated in a 96 well coverglass bottom dish (#655891, Greiner). Total EGFP-SM1A signal was collected for 16 positions per well. Then, triton buffer (5 uM PEG800, 100 mM PIPES, 150 mM NaCl, 1 mM EGTA, 1 mM MgCl2, .5% triton, 90% H20) was added to permeabilize the cells and release soluble EGFP-SM1A. The exact same positions were re-imaged to collect the triton-insoluble EGFP-SM1A signal. Individual cells masked were manually identified using FIJI. Local background fluorescence and mean fluorescence intensity was measured for each cell before and after permeabilization. Fraction assembled was then calculated as background subtracted signal post-permeabilization relative to background subtracted signal pre-permeabilization.

Statistics

Statistics were performed using the GraphPad Prism. Specific tests used for each experiment are stated in figure legends. Asterisks are used to convey statistical significance are as follows: * for $p < 0.05$, ** for $p < 0.005$, *** for $p < 0.0005$.

Results

Reported Mutation R1275L Associated with Vascular Disease

MYH11 mutations have been shown to be correlated with increased risk of thoracic aortic aneurysm and dissection (TAAD) in families who are afflicted. One of such mutations is the R1275L substitution. This mutation in the coiled-coil region of the protein segregated with TAAD and/or PDA (patent ductus arteriosus) in families with the mutation. [3,90]

Because this mutation is located within the tail region of the protein which is important for filament formation and dynamics, we hypothesized dynamics may be altered by this mutation. The mutation in the tail region may interrupt electrostatic interactions between monomers, or it may impede folding of the monomer into the self inhibited form, or both. It is conceivable that both slower and faster dynamics, and over and under-assembly of smooth muscle myosin could predispose a patient. The aorta serves as a shock absorber; as blood is pumped at a high velocity from the left ventricle and encounters the sharp turn of the aorta, it is important that the aorta must be able to both flex to absorb pressure and contract to counteract pressure. Slower exchange or over-assembly may both produce an effect in which the smooth muscle is perpetually in a tenser state and stiffened. This stiffening can impede the aorta's ability to both flex and contract, setting up a weak area within the vessel that is exposed to high pressure, a ticking time bomb for aneurysm and dissection. Conversely, faster exchange or under-assembly may leave vascular smooth muscle without the ability to produce sufficient force to help counteract the pressure of blood flow from the left ventricle. This could also lead to weakness in the aorta, and a propensity to fail over time.

While many mutations have been found to be associated with disease, careful cell biology analysis of the changes that occur are lacking. Phenotype is known, genotype is known, but how exactly the genotype leads to phenotype is often unclear. This leaves patients and their families

with little to no option for treatment other than a “watch and see” approach where patients are monitored through ultrasound for changes in aortic diameter. Then only when the aneurysm reaches considerable size (often 5 cm) is surgery performed to reinforce the vessel. The surgery is a difficult surgery, often with a long recovery, but the only treatment to prevent aneurysm or rupture.

With a greater understanding of how mutations affect cell biology, the course of treatment may eventually be able to be amended. By recognizing mutations in different regions of the myosin with similar defects in dynamics or assembly, we can start to develop an alternative treatment. For instance, if mutations in predictable regions of the smooth muscle myosin tail consistently under-assembly and fail to contract appropriately, starting a patient on a smooth muscle myosin activator may increase vascular health long term.

Reported Mutation R1275L Alters Filament Dynamics

To investigate the change the R1275L mutation, previously reported to be a disease causing mutation, may have on filament dynamics FRAP was performed. FRAP was performed similarly to Chapter 3’s investigation into wild type SM1A dynamics. A7R5 cells were transformed with the EGFP-SM1A-R1275L plasmid to overexpress the mutant smooth muscle myosin isoform. 24 hours after transfection and plating, FRAP was performed. In this way, we can measure exchange between monomeric and filamentous populations of myosin.

Figure 15 displays an example cell expressing EGFP-SM1A-R1275L with insets showing bleach region and recovery. FRAP quantification includes the mobile fraction, which is the fraction of filamentous SM1A exchanging, and the t ½, which is the time it takes for half of the total exchange to occur. Our data suggests that while mobile fractions are comparable (Fig 5.1B)

, t ½ (Fig. 15C) is increased and k_{off} (Fig 15D) is decreased for EGFP-SM1A-R1275L compared to WT. This indicates that in smooth muscle myosin filaments with the 1275L mutation, the same amount of myosin is exchanged as in WT filaments, however it is taking longer to do so. This may be due to a lower affinity for forming filaments because of the mutation in the tail region. The R1275L mutation affects the speed at which exchange occurs in smooth muscle myosin filaments.

This decrease in k_{off} and increase in t ½ could alter the levels of WT and mutated smooth muscle myosin in the filaments. A decrease in k_{off} represents a decrease in the exchange rate of myosin monomers in and out of the filaments. However, whether this overall rate being decreased is a result of a decrease rate of myosin moving on or off the filament is difficult to decipher, with different potential molecular mechanisms. If the decrease in k_{off} is a result of a decrease in mutated myosin moving off of the filament, this indicates that the mutated myosin is more stable within the filament than the WT. This would bias the system towards having a larger percentage of mutated myosins within a filament compared to WT myosins.

However, the decrease in k_{off} could also be a result of a slower on rate, or a slower rate of mutated myosins joining the filament. This would have the opposite effect, where the system would be biased towards a more WT filament than a mutated filament. However, this lesser affinity to join a filament may result in filaments containing more WT smooth muscle myosin, but smaller or fewer assembled filaments overall.

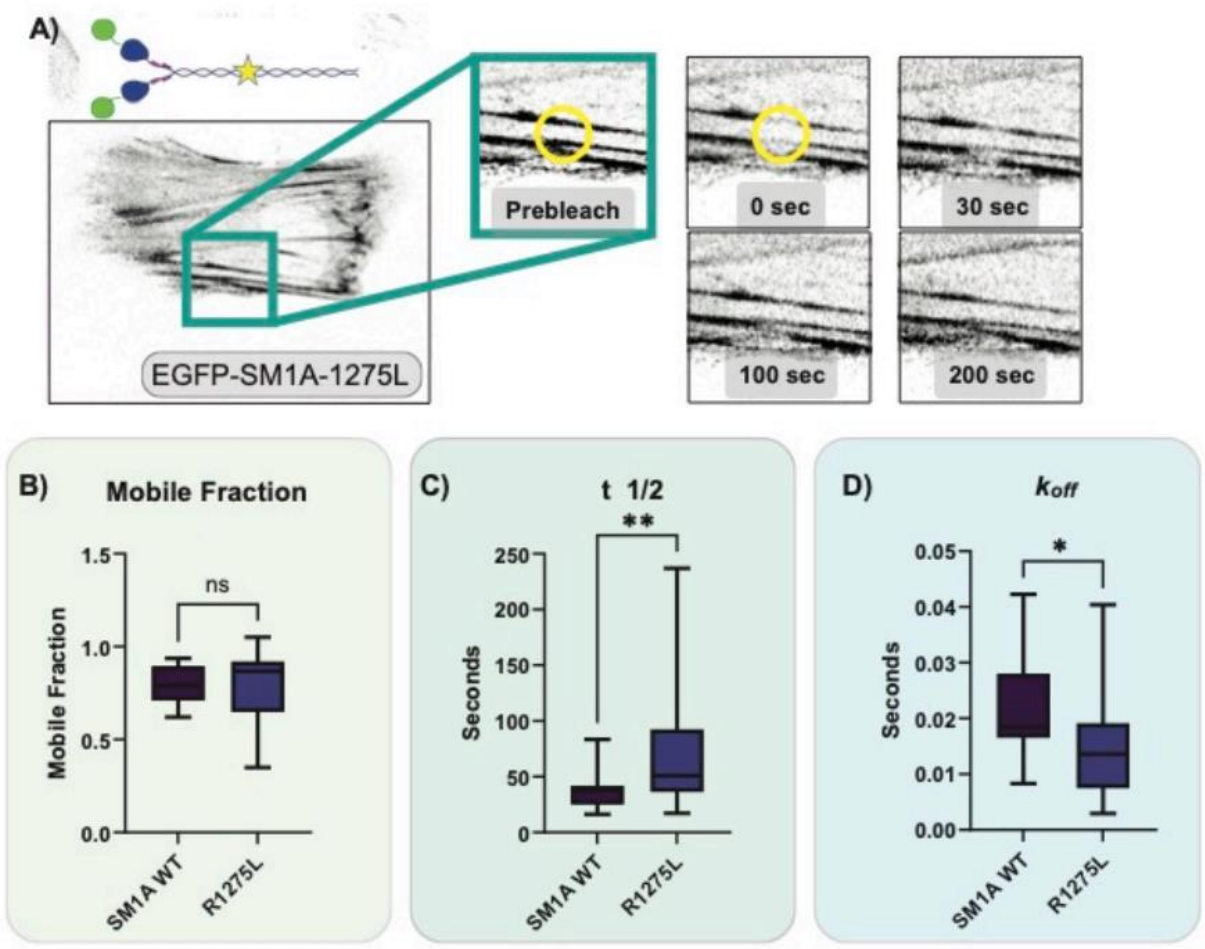

Figure 16. Dynamics are Altered in SM1A-R1275L Mutants. A) FRAP example A7R5 expressing EGFP-SM1A-R1275L. Bleach region indicated by green circle in insets. Schematic displays smooth muscle myosin monomer with a star at the approximate region of R1275L mutation.B & C) Mobile fraction (B) t 1/2 (C) and k_{off} (D) plotted for EGFP-SM1A-R1275L expressing A7R5 cells from 3 experiments.

In heterozygous patients, assuming allelic balance, half of the total smooth muscle myosin would be WT and half would be mutant myosin. More than half of total myosin is assembled at steady state (Fig. 13), meaning that even at steady state, filaments of WT myosin alone would be insufficient to produce a baseline level of contraction. Thus, SM1A-R1275L myosin being slower or less likely to be incorporated into filaments, must affect assembly levels

and contractility at steady state and, to a greater degree, upon activation.

Reported Mutation R1275L Alters Filament Assembly

To investigate EGFP-SM1A-R1275L assembly, we performed a single-cell imaging-based triton permeabilization assay to measure populations of monomeric and filamentous myosin. This assay was nearly identical to the assay performed in Chapter 4, with a different cell line used. To better measure potentially minor changes in smooth muscle myosin assembly defects caused by the mutation, we turned to a fibroblast cell line (JR20) which has non-muscle myosin 2A knocked out. This leaves a cell line with little myosin of any kind present. Using this cell line allowed us to examine the assembly of SM1A and EGFP-SM1A-R1275L in a sort of vacuum. In a system devoid of myosin, there is little change for creation of heterofilaments with WT and EGFP-SM1A-R1275L, or EGFP-SM1A-R1275L and non-muscle myosin.. Therefore, we can measure assembly plainly and without confounding or complicating factors.

NM2A KO expressing EGFP-SM1A-R1275L were imaged to measure total EGFP-SM1A-R1275L intensity, permeabilized with a triton buffer to remove monomeric EGFP-SM1A-R1275L pool, and re-imaged to measure remaining filamentous signal (Fig. 17A & 17B). Comparing intensity differences pre- and post-triton enables quantitative determination of monomer/filament ratios on a single cell basis.

Fraction of myosin assembly was measured at steady state (in the absence of contractile stimuli) in JR20 NM2A KO cells expressing the WT EGFP-SM1A and EGFP-SM1A-R1275L (shown schematically in Fig. 17) and is plotted as shown (Fig. 17). Individual dots represent each cell, colors represent biological replicates, and larger dots represent the mean for each biological replicate. Fractions of smooth muscle myosin (SM1A) assembled at around 75%, a similar

percentage to the fraction of smooth muscle myosin assembled in the A7R5 cells. This helps to validate the model system used, as the controls are largely unchanged. When looking at assembly in the EGFP-SM1A-R1275L mutation however, assembly is altered.

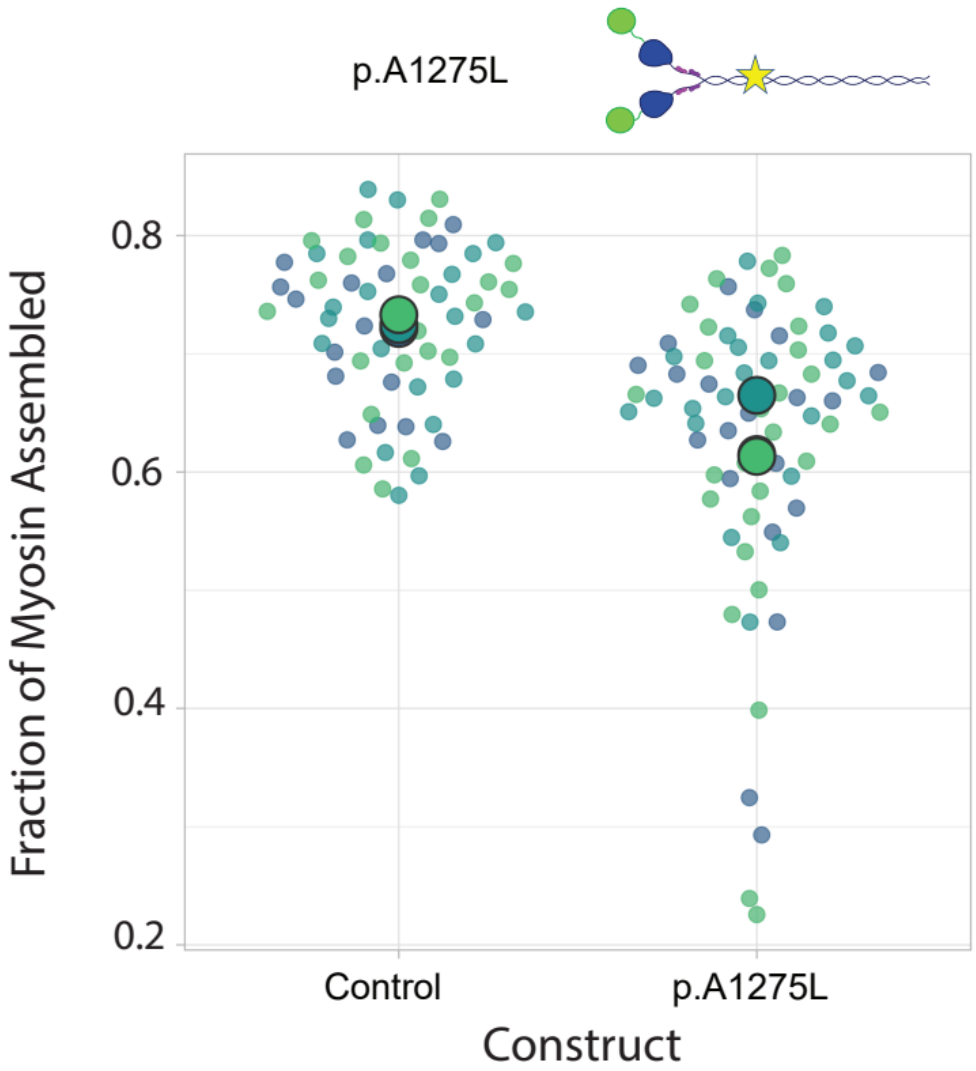

Figure 17. Smooth Muscle Myosin Filament Assembly is Impaired in EGFP-SM1A-R1275L. Quantification of the fraction of SM1A assembled in control cells and cells expressing EGFP-SM1A-R1275L. Small circles indicate individual cells. Larger dark circles indicate means of three independent experiments. t-tests were performed comparing the mutant group to the control.

Assembly is markedly decreased when the R1275L mutation is present. This under-assembly may hint at an underlying cause for the TAAD phenotype present in patients. As mentioned before, under-assembly may contribute to a defect in force production, eventually leading to a weakened aorta prone to aneurysm and dissection. Additionally, this data is at steady state, but what remains unknown is how the mutation impacts the necessary filament building response to a contractile stimulus. This mutation may impede a VSMC ability to increase filaments in a timely manner in response to a contractile stimulus, amplifying the under-assembly defect.

Novel Mutation Identified in Patient

Our collaborator, Dr. Greg Aubert (MD/PhD), has a patient with a familiar history of TAAD, and upon sequencing, found a mutation in the MYH11 gene. It is significant to note that a variety of other potential genes were all sequenced and no other changes or mutations were found, suggesting it is the MYH11 mutation that may be contributing to or causing disease. This mutation has not previously been reported in the literature, and therefore is not yet classified as a pathology associated mutation. However, through sequencing of the patient and the family, it is clear that this mutation may play a role in predisposing individuals to vascular disease. Figure 18 shows the pedigree of the patient, illustrating the penetration this mutation has in affecting disease course. This patient and their family follows the trend of many other MYH11 mutations where profound vascular disease occurs within the family at a much higher rate than the general population. This pedigree also illustrates many unknowns of patients with MYH11 mutations. These mutations may present slightly differently in each person, including severity of vascular disease and outcome. Because penetrance and severity of disease can vary, often patients who

have relatives with profound vascular disease are left wondering where their own health stands. Without understanding the molecular and cellular mechanisms behind this, patients are left to worry and wait in the unknown.

The mutation found was p.R1849V which is within the latter portion of the coiled-coil tail region. While in a different region of the tail than the p.R1275L mutation, this novelly reported mutation again was within the coiled-coiled region. Because this mutation has the potential to affect electrostatic interactions between myosin monomers forming filaments, we analyzed filament dynamics and assembly using FRAP and the single cell imaging based assay.

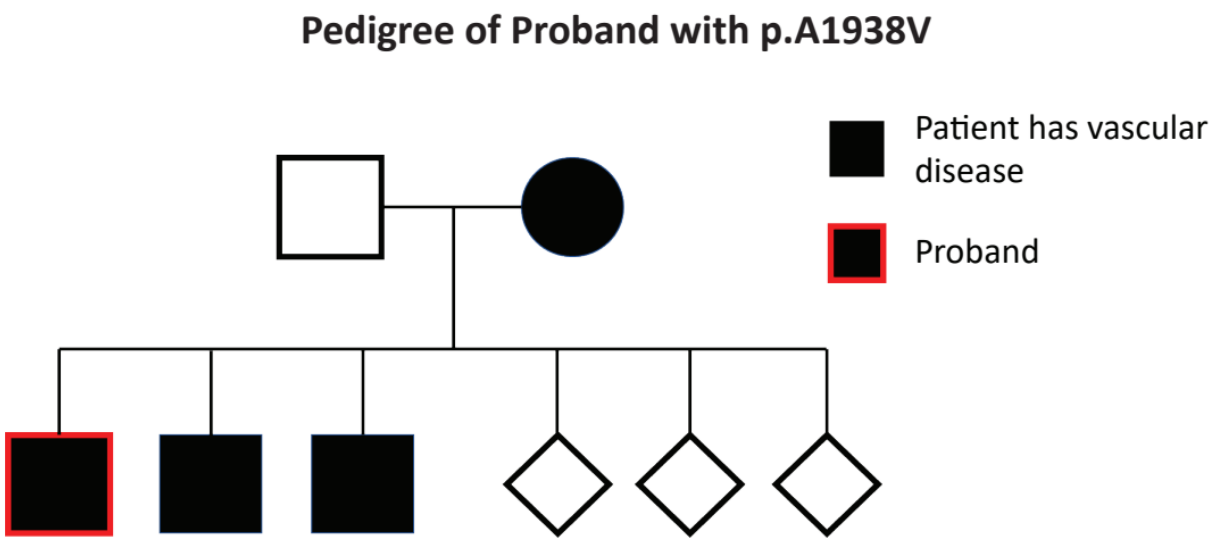

Figure 18. Pedigree of Patient with Novel p.A1839V Mutation. The patient seen in the clinic, the proband, is shown with a red outline. Black-filled shapes indicate presence or suspicion of vascular disease.

Novel Mutation A1839V Alters Filament Dynamics

First, we performed FRAP in an identical manner to previously described above. We used A7R5 cells 24 hours after being transfected and overexpressing EGFP-SM1A-A1839VL

(shown schematically in Fig. 19). A region was photobleached and recovery watched to determine how much of the smooth muscle myosin in the filament was exchanging and how rapidly it occurred. Figure 5.4A shows an example of FRAP performed, with insets illustrating recovery of EGFP-SM1A-A1839V. Note that there does not to be an immediate visible difference between cells expressing WT SM1A and SM1A-A1839V. At face value the mutated smooth muscle myosin seems to be capable of forming normal looking filaments. In measuring mobile fraction (Fig 19B) and t ½ (Fig 19C), we found the mobile fraction is decreased in the mutant construct. To further determine kinetics of exchange, we measured k_{off} in both WT and mutant constructs (Fig 19D). There was no significant difference in k_{off} between the constructs. A lower mobile fraction, combined with unchanged t ½ and k_{off} indicates that myosin is exchanged within the filaments at a similar time when the 1839V mutation is present, however, less myosin overall is exchanged.

Less myosin being exchanged may result in a variety of effects. The patient with this mutation is heterozygous, meaning that both WT and A1839V mutated smooth muscle myosin is present. Presumably, together these form heterofilaments comprised of both mutated and WT myosin. If less A1839V mutated smooth muscle myosin is being exchanged, over time that may lead to a greater level of mutated myosin within the filaments, therefore producing an outsized effect on SMC contraction overall.

Novel Mutation p.A1839V Alters Filament Assembly

To assess a potential impact that the mutation may have on filament assembly, the single cell imaging based assembly assay was used to quantify both monomeric and filamentous populations of smooth muscle myosin. NM2A KO expressing EGFP-SM1A-A1839V were

imaged to measure total EGFP-SM1A-A1839V intensity, permeabilized with a triton buffer to remove monomeric EGFP-SM1A-A1839V pool, and re-imaged to measure remaining filamentous signal (Fig. 20). Comparing intensity differences pre- and post-triton enables quantitative determination of monomer/filament ratios on a single cell basis.

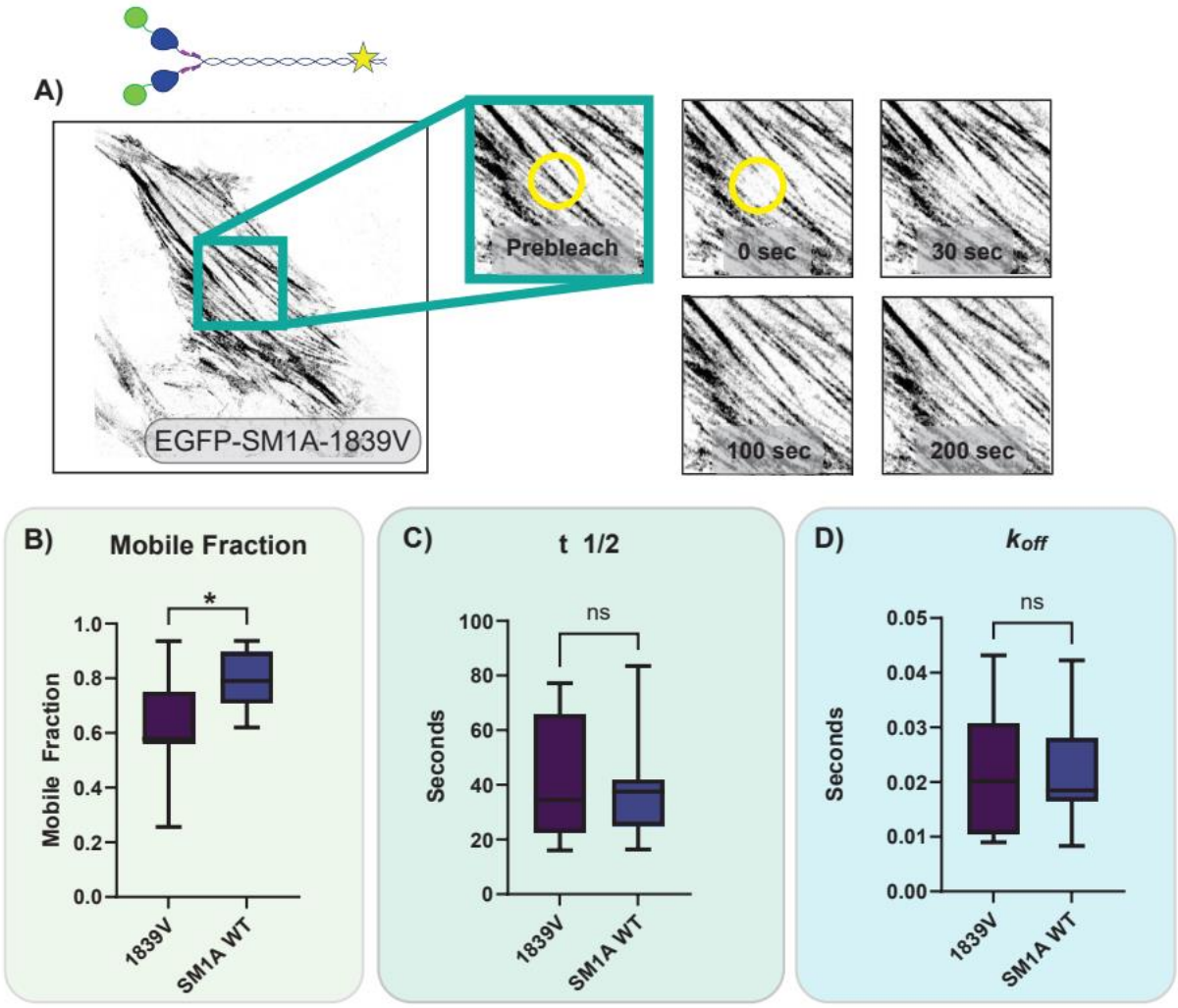

Figure 19. Dynamics are Altered in SM1A-A1839V Mutants. A) FRAP example A7R5 expressing EGFP-SM1A-A1839V. Bleach region indicated by yellow circle in insets. Schematic displays smooth muscle myosin monomer with a star at the approximate region of A1839V mutation. B & C) Mobile fraction (B) t 1/2 (C) and k off (D)plotted for EGFP-SM1A-1839V expressing A7R5 cells from 3 experiments.

Fraction of myosin assembly was measured at steady state in JR20 NM2A KO cells expressing the WT EGFP-SM1A and EGFP-SM1A-A1839V (shown schematically in Fig. 20) and are plotted as shown (Fig. 20). Individual dots represent each cell, colors represent biological replicates, and larger dots represent the mean for each biological replicate. Similarly to the R1275L mutation, in the EGFP-SM1A-A1839V mutation however, assembly is altered. Fraction of myosin assembled in cells expressing EGFP-SM1A-A1839V is decreased, by even a touch more than in the R1275L mutation. This is significant because, as stated before, this underassembly may cause a defect in contractility and therefore contribute to disease phenotype.

Overall, the two mutations in the tail regions studied both caused a defect in assembly and decreased the overall fraction of myosin assembled. This may hint towards a trend, where mutations disrupting the coil-coil formation or disrupting the electrostatic along the tail between monomers may alter overall filament assembly.

Filament Assembly is Unchanged with Overexpression

To confirm the alterations in fraction of myosin assembled seen in the R1275L and A1839V mutations are not due to changes in expression of the construct, fluorescence intensity and myosin assembly was plotted. Mean fluorescence intensity of the whole cell was plotted against the fraction of myosin found to be assembled in that cell. This was done for cells expressing EGFP-SM1A (Fig. 21A), EGFP-SM1A-R1275L (Fig. 21B), and EGFP-SM1A-A1839V (Fig. 21C). Each dot represents measurement from a single cell. In each graph it is clear there is no association between mean fluorescence intensity and fraction of myosin assembled.

Similarly, mean fluorescence intensity is similar between the three constructs. Together this indicates that expression of each construct is at a similar level. Beyond that, overexpression

of the construct does not affect filament assembly. More or less GFP tagged smooth muscle myosin has no bearing on the amount of myosin assembled into filaments. This helps to confirm the alterations in assembly between the constructs is due to the mutations, and not changes in overexpression or smooth muscle myosin quantity.

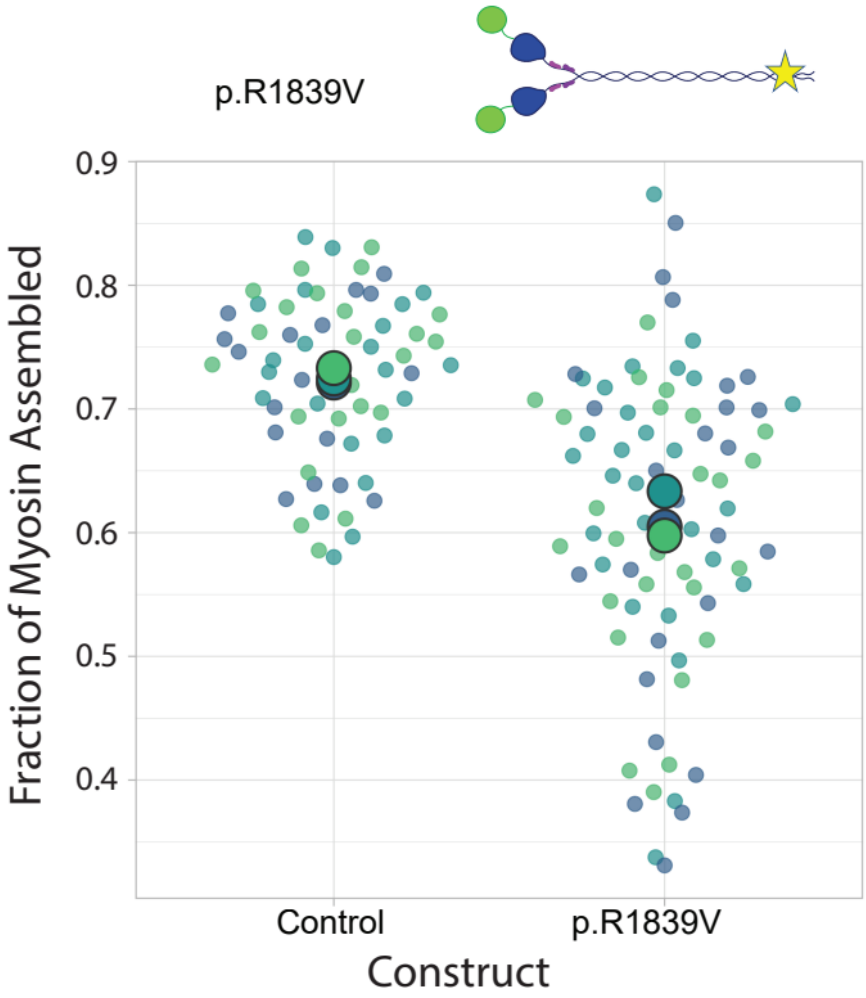

Figure 20. Smooth Muscle Myosin Filament Assembly is Impaired in EGFP-SM1A-A1839V. Quantification of the fraction of SM1A assembled in control cells and cells expressing EGFP-SM1A-A1839V. Small circles indicate individual cells. Larger dark circles indicate means of three independent experiments. t-tests were performed comparing the mutant group to the control.

Summary and Discussion

The importance of the alterations in dynamics remains unclear, and there are mysteries remaining. We are measuring changes on the time scale of seconds; however, patients often experience vascular disease decades into life. This time scale is an important disconnect that we have been unable to solve. If MYH11 mutations impart an inability to properly contract, and that alone caused TAAD, it would be expected that then vascular dysfunction would occur earlier in life (infancy even) than is seen in patients. It is conceivable that these changes, played out of the tissue level scale and over time, can alter the properties of vascular smooth muscle, including stiffness and contractility. Many changes that occur during aging may occur earlier and to a greater decree in tissues with MYH11 mutations. Contractile defects and stiffening both occur with aging.[116,117] Increasing aortic stiffness has been shown to be a significant risk factor for vascular disease and is associated with worsened patient outcomes. [118–120] Changes in myosin dynamics and assembly, may mimic and accelerate changes than occur in normal aging, causing premature changes in tissue properties and putting patients at an increased risk for disease.

While the number of reported smooth muscle myosin mutations causing TAAD is low, this number is most likely a gross underreporting. Patients who present with TAAD worldwide are rarely sequenced, so the exact impact MYH11 mutations have on increased incidence of TAAD is impossible to know at this point.

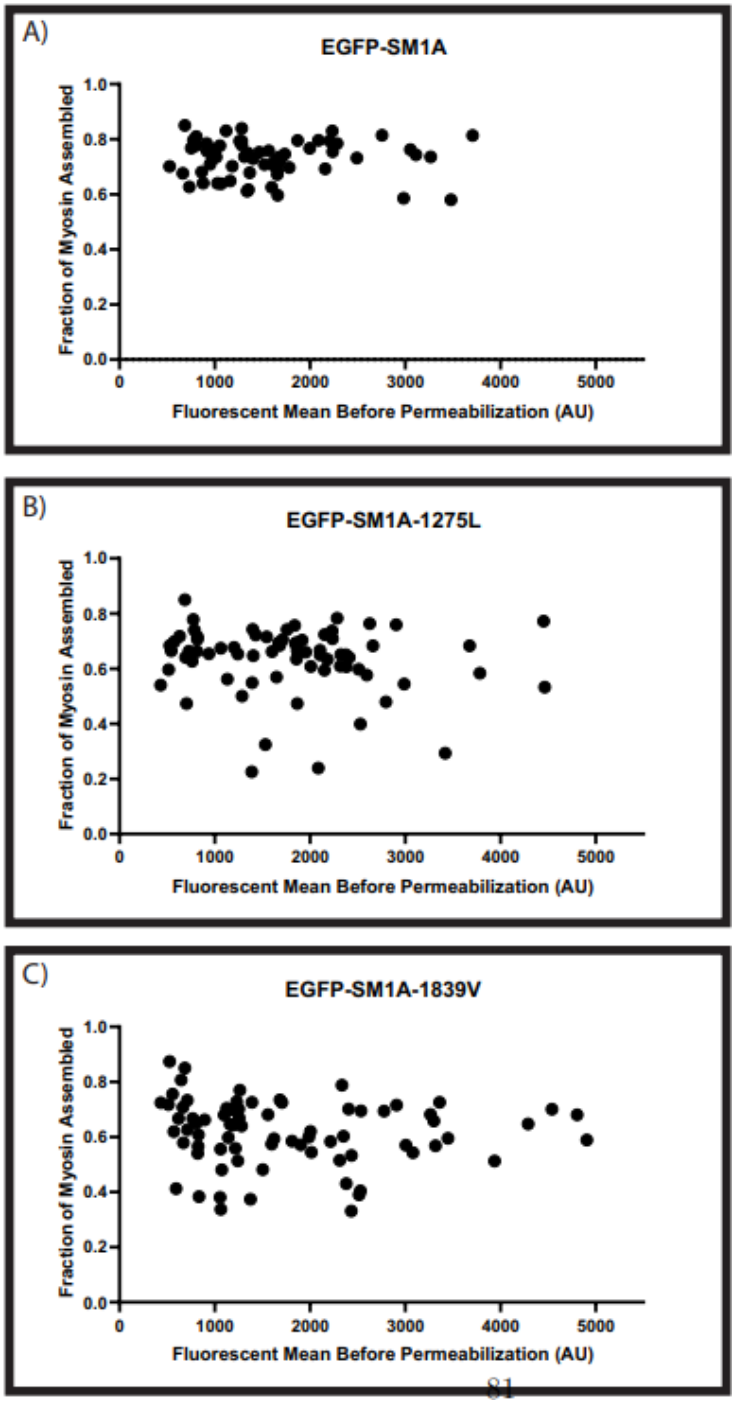

Figure 21. Fluorescent Mean vs Fraction of Myosin Assembled. Each dot represents a single cell from three separate experiments.

While we have only investigated two MYH11 mutations, we have hopefully added to the overall understanding of how specific mutations can affect smooth muscle myosin assembly and dynamics. As more information is gathered the field can not only observe how mutations affect myosin and cellular function, but also predict this information. With predicting how a patient's mutation may affect how their smooth muscle may behave, targeted therapy can occur.

CHAPTER 6

SUMMARY AND DISCUSSION

My research leads to an updated model of SM1A filament assembly and contraction (Fig. 22). At steady-state, SM1A forms highly dynamic filaments with most, but not all of the SM1A in the filamentous state. Additionally these filaments are likely co-assembled with NM2, with the heterofilaments also being highly dynamics. We speculate that at steady-state, a portion of SM1A is in the filamentous IHM state, as the increase in force production after activation is greater than the increase in filament assembly, indicating that force production is due to both activation of existing filaments and assembly of new filaments. Upon SMC activation, elevated cytosolic calcium activates MLCK to phosphorylate RLC. This leads to unfolding of the 6S monomers into assembly competent 10S that assemble into new filaments, increasing overall filamentous SM1A, decreasing monomeric populations, and decreasing exchange kinetics. In parallel, we speculate that MLCK phosphorylates RLC in filamentous IHM, enhancing activation of those existing filaments to drive physiological levels of contraction.

Smooth Muscle Myosin Filament Dynamics Summary

Our data is the first to investigate SM1A dynamics in cells. We observe rapid exchange kinetics between monomers and filaments. Considering the genetic similarity to NM2, this is not surprising. However, considering the function of SM1A is largely to drive uni-axial contractile events, similar to striated myosin 2s, the rationale for rapid exchange kinetics is not immediately apparent.

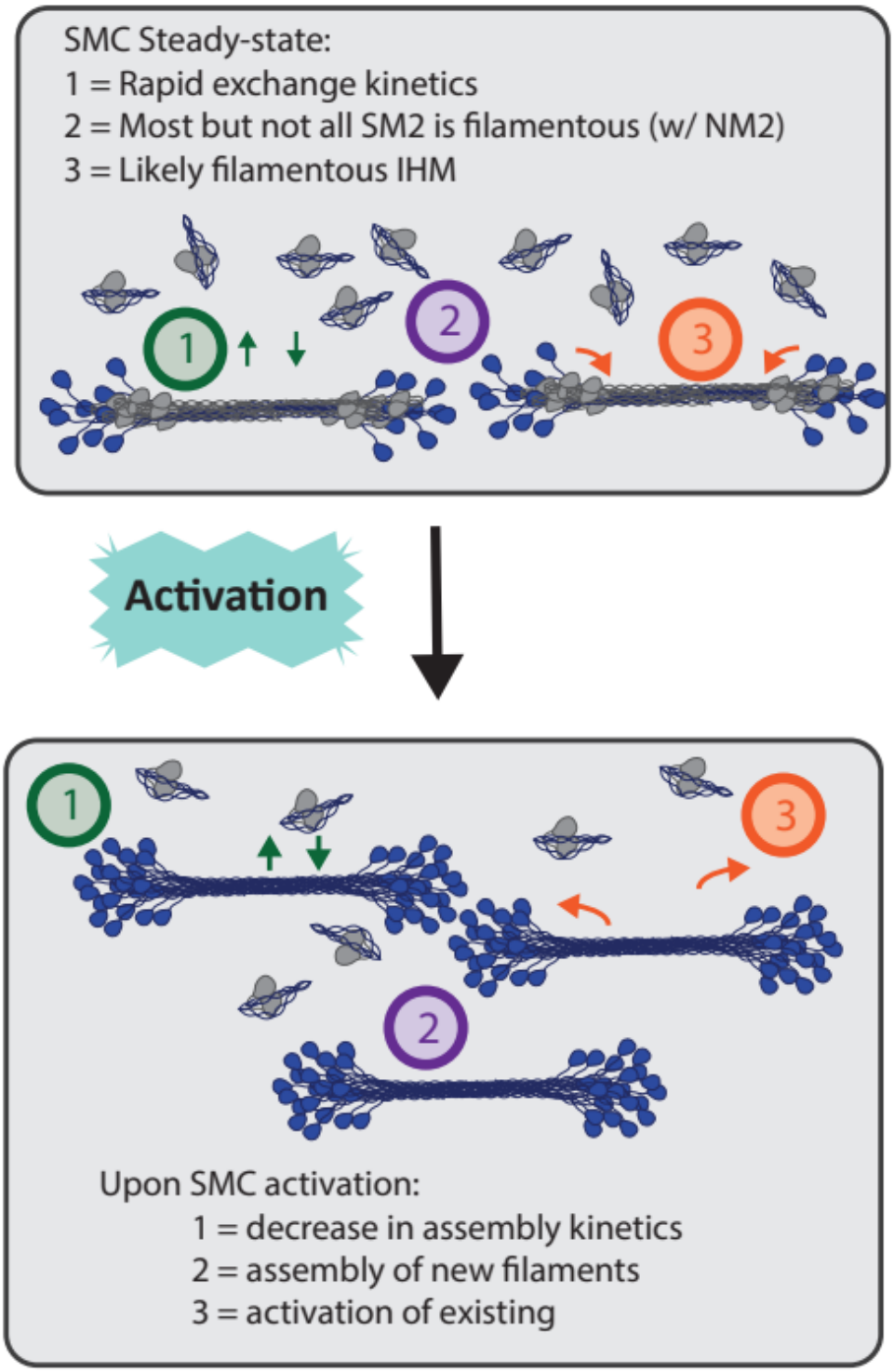

Figure 22. Model of SM1A Assembly at Steady-State and Upon Activation. See text for description.

In future studies, it will be important to determine exchange kinetics of endogenous SM1A in primary SMCs, ideally in intact tissue or organisms. This is obviously significantly more challenging than our current model system. Should similar exchange kinetics be observed in these future experiments, we speculate that rapid exchange kinetics enable rapid and tunable assembly levels that tune force production. Requisite changes in blood pressure or vascular tone could be rapidly achieved by modulating SM1A activation and assembly to a new setpoint.

Extracting more molecular level assembly information from our FRAP data during induced contraction is challenged by the timescales at play. During induced contraction, we observed a longer t ½ and shorter k_{off}, indicative of reduced exchange kinetics. However, we also observed a larger mobile fraction, which indicates a greater fraction of total SM1A exchanging. In our other experiments, cytosolic calcium, SM1A assembly, and traction forces all peak within 1-2 minutes of carbachol-induced activation, after which they decay to steady-state levels within minutes. However, plateaus in our carbachol-treated FRAP data (required to fit exponential curves) require observation for ~5-10 minutes. Therefore, the SM1A networks in our bleach regions are likely experiencing some exchange, as expected, but also significant filament assembly and subsequent disassembly, all within the experimental window. This complicates interpretation, but, overall, paints a picture of an SM1A filamentous network that is dynamic and responsive to SMC activation state. Future experiments using single molecule tracking of individual SM1A monomer lifetimes in filaments should enable the temporal resolution required to fully elucidate changes in exchange kinetics throughout an induced contraction event.

Smooth muscle functions in organs throughout the body, with each organ placing unique demands on the resident SMCs. For example, vascular smooth muscle performs tonic contraction

to maintain vessel tone while gastrointestinal smooth muscle performs phasic contraction to move food through the GI tract. [121] Splice variants of SM1A lead to unique SM1A isoform expression in different SMCs. [122] Therefore, it would be interesting to determine if SM1A isoforms have unique exchange kinetics and assembly levels, and if these correlate with contractile properties of the SMCs in which they are expressed. Complicating this, of course, is the presence of NM2 isoforms and splice variants in each SMC population [101] that could also contribute to variation in contractile properties, especially if SM1A and NM2 are co-assembling. Further complexity could also arise from heterogenous myosin 2 subcellular functions within SMCs, as recent evidence demonstrated unique subcellular localization for SM1A and NM2 in freshly isolated primary cells. [123] Finally, while the structure of an NM2 bipolar filament in cells is relatively well-established, the precise structural features of SM1A filaments in intact cells and tissues remains an active area of debate. [124] Future studies to dissect unique and common biophysical properties of SM1A and NM2 filaments in SMCs should prove insightful.

Smooth Muscle Myosin Filament Assembly Summary

Elucidating the amount of myosin assembled at baseline and contraction, and the kinetics of how assembly increases, is critical to understanding smooth muscle contraction as a whole. Smooth muscle contraction is not nearly as well characterized as striated muscle contraction. Therefore, there may be aspects of contraction that may be modulated to affect physiology that are not currently being targeted. Smooth muscle contraction plays such an important role in physiology, and furthermore dysregulation of contraction drives a variety of pathologies. Increased vascular tone plays a role in high blood pressure, and our current understanding of SMC contraction has limited our ability to treat this disease. By furthering our knowledge of

SMC contraction, we can better understand normal physiology and open up therapeutic targets for disease.

Understanding the degree of filament assembly at a given time not only helps to further understanding of SMC contraction as a whole, but provides an important baseline to compare the effects of a variety of mutations and drugs.

Establishing baseline levels of assembly of the SM1A isoform lays the foundation to explore differences in isoform, mutations, and the effects different drugs may have. There are four isoforms of smooth muscle myosin - each of which may have unique assembly levels. Isoforms SM1 and SM2 differ in inserts along the tail region, and it would follow that these differences may impart differences in basal assembly levels or assembly responses to activation. Examining these differences may aid in explaining to wide variety of contraction patterns that smooth muscle exhibits throughout the body using the same motor protein.

Assembly levels are altered in cells expressing smooth muscle myosin with both mutations examined here. These assembly defects may contribute to disease phenotype by producing contractile deficits in the cells. This is an important finding that may be able to be translated to a variety of different mutations. By using a similar assay, and testing assembly using different pathology associated mutations, a catalog could be developed. Developing a catalog of mutation and effects on assembly would allow for potential genotypte/phenotype patterns to emerge, where specific mutations and/or locations lead to overassembly/ underassembly. In the future, this would allow clinicians to to potentially predict the effect of the mutation present on tissue level contractility and to treat accordingly.

Smooth Muscle Myosin Mutations Alter Assembly and Dynamics – Summary

Understanding and appreciating how myosin mutations may drive disease is vital for development of new therapeutic targets. This has certainly been true in cardiac pathologies. By first identifying cardiac myosin mutations in patients with hypertrophic cardiomyopathy, and later understanding these mutations result in a hypercontractile myosin, the door has been opened for new targets to treat a previously uncontrolled disease. By screening patients, the presence and prevalence of mutations producing hypercontractile cardiac myosins was assessed. Then by careful analysis of how hypercontractile myosins or overly activated myosins led to disease, the path was paved to develop a drug that could counteract this increase in contractility by directly inhibiting myosin's behavior.

Enter Mavacamten - the cardiac muscle myosin inhibitor that has been proven successful in clinical trials of not only impacting cardiac muscle contractility, but impacting patient outcomes. In this sense, the development and use of Mavacamten has proven that identification and characterization of pathology associated mutations in myosin can lead to profound effects on health and the treatment of disease. While the cardiac field has had a head start in this, there is all the reason to believe the same story could play out in smooth muscle- that by identifying and characterizing smooth muscle myosin mutations, we could uncover novel therapeutic targets and help to fill a gap in treatment.

Recent advances in cardiomyopathy-driving myosin mutations (primarily MYH7) suggest some mutations are either stabilizing or destabilizing the IHM to create hyper or hypo-contractile systems. [51] Some pathologies driven by mutations in the NM2A heavy chain, collectively termed MYH9-Related Disease, are found along the coiled-coil tail and are thought

to disrupt filament assembly and dynamics. [125,126] Together this suggests it is highly likely that there exist a wide variety of smooth muscle myosin mutations associated with aortic dysfunction and disease that are altering myosin assembly and dynamics.

Many pathogenic or likely-pathogenic SM1A mutations have been reported [4], often resulting in aortic dysfunction, but most have not received any mechanistic scrutiny. Our work has scratched the surface of understanding how mutations may impact filament assembly and dynamics. This is an important first step in proving that disease associated mutations can have profound and measurable effects. Our results indicate that there is an under-assembly of smooth muscle myosin with either mutation (R1275L and A1839V) present. This under-assembly may be more profound when SMCs are activated, indicating these SMCs are incapable of appropriately producing a contractile response. By measuring assembly and traction forces after activation in both mutations, I could investigate changes in assembly and potential impacts on force production. Understanding these mutations better, and how the molecular changes we observe could lead to pathophysiology, is a vital step forward in the end goal of improved patient care. By understanding if and when mutations increase or decrease force, we could better target disease causing processes.

As both hyper- and hypo-contractile SMCs could alter tissue compliance or tunability in an unfavorable manner, increasing or decreasing overall SM1A assembly and activity could drive pathology. Future studies to carefully dissect SM1A mutation impact on SM1A assembly dynamics should prove insightful. By characterizing mutations more carefully, precision medicine may be possible for patients with this rare genetic cause of cardiovascular disease. People with mutations impeding filament assembly and causing instability may be given smooth

muscle myosin activators to combat hypocontractility, and the reverse may be true for mutations causing over-assembly or hypercontractility. While this would be many, many years down the road, it is not inconceivable to think closer molecular analysis of mutations may help pave that road.

I have studied two mutations, we speculate that many more of these SM1A mutations are altering IHM stability and/or altering filament assembly. My work underlies the importance of not only studying the molecular mechanisms behind pathology associated mutations, but also the great value of genetic sequencing of patients. Because aortic dissection is swift and often presents as a trauma to the emergency department, the doctors treating this are often, and rightly, focused of preserving life. However, in follow up, greater effort to sequence patients may help to parse out the contributions of environmental and genetic factors to aortic disease. A broader database of mutations would allow for a more robust study of molecular changes to myosin, and the physiological impacts at the tissue and human level.

Overall, our studies provide foundational details for SMC physiology and contraction, including highly dynamic filaments where both filament activation and filament assembly contribute to force production. Both dynamics and filament assembly are demonstrably modulated, and our studies open the door into elucidating precise and unexplored mechanisms (e.g. heavy chain phosphorylation) for both normal physiology and pathophysiology.

REFERENCE LIST

1. Zhuge Y, Zhang J, Qian F, Wen Z, Niu C, Xu K, et al. Role of smooth muscle cells in Cardiovascular Disease. Int J Biol Sci. 2020;16: 2741–2751.

2. Yokoyama U, Arakawa N, Ishiwata R, Yasuda S, Minami T, Goda M, et al. Proteomic analysis of aortic smooth muscle cell secretions reveals an association of myosin heavy chain 11 with abdominal aortic aneurysm. Am J Physiol Heart Circ Physiol. 2018;315: H1012–H1018.

3. Pannu H, Tran-Fadulu V, Papke CL, Scherer S, Liu Y, Presley C, et al. MYH11 mutations result in a distinct vascular pathology driven by insulin-like growth factor 1 and angiotensin II. Hum Mol Genet. 2007;16: 2453–2462.

4. Takeda N, Komuro I. Genetic basis of hereditary thoracic aortic aneurysms and dissections. J Cardiol. 2019;74: 136–143.

5. Li M, Li S, Rao Y, Cui S, Gou K. Loss of smooth muscle myosin heavy chain results in the bladder and stomach developing lesion during foetal development in mice. J Genet. 2018;97: 469–475.

6. Brown BA, Williams H, George SJ. Chapter Six - Evidence for the Involvement of Matrix-Degrading Metalloproteinases (MMPs) in Atherosclerosis. In: Khalil RA, editor. Progress in Molecular Biology and Translational Science. Academic Press; 2017. pp. 197–237.

7. Hunt JM, Graham BB. Pulmonary Hypertension/Pulmonary Arterial Hypertension. In: McManus LM, Mitchell RN, editors. Pathobiology of Human Disease. San Diego: Academic Press; 2014. pp. 2625–2635.

8. Touyz RM, Alves-Lopes R, Rios FJ, Camargo LL, Anagnostopoulou A, Arner A, et al. Vascular smooth muscle contraction in hypertension. Cardiovasc Res. 2018;114: 529–539.

9. Berair R, Hollins F, Brightling C. Airway smooth muscle hypercontractility in asthma. J Allergy . 2013;2013: 185971.

10. Zhang W, Cheng Z, Qu X, Dai H, Ke X, Chen Z. Overexpression of myosin is associated with the development of uterine myoma. J Obstet Gynaecol Res. 2014;40: 2051–2057.

11. Chamley-Campbell J, Campbell GR, Ross R. The smooth muscle cell in culture. Physiol Rev. 1979;59: 1–61.

12. Poole JC, Cromwell SB, Benditt EP. Behavior of smooth muscle cells and formation of extracellular structures in the reaction of arterial walls to injury. Am J Pathol. 1971;62: 391–414.

13. Frismantiene A, Philippova M, Erne P, Resink TJ. Smooth muscle cell-driven vascular diseases and molecular mechanisms of VSMC plasticity. Cell Signal. 2018;52: 48–64.

14. Chamley JH, Campbell GR, Burnstock G. Dedifferentiation, redifferentiation and bundle formation of smooth muscle cells in tissue culture: the influence of cell number and nerve fibres. J Embryol Exp Morphol. 1974;32: 297–323.

15. Kocher O, Gabbiani F, Gabbiani G, Reidy MA, Cokay MS, Peters H, et al. Phenotypic features of smooth muscle cells during the evolution of experimental carotid artery intimal thickening. Biochemical and morphologic studies. Lab Invest. 1991;65: 459–470.

16. Virmani R, Kolodgie FD, Burke AP, Farb A, Schwartz SM. Lessons from sudden coronary death: a comprehensive morphological classification scheme for atherosclerotic lesions. Arterioscler Thromb Vasc Biol. 2000;20: 1262–1275.

17. Bennett MR, Sinha S, Owens GK. Vascular Smooth Muscle Cells in Atherosclerosis. Circ Res. 2016;118: 692–702.

18. Davies MJ, Thomas A. Thrombosis and acute coronary-artery lesions in sudden cardiac ischemic death. N Engl J Med. 1984;310: 1137–1140.

19. Huxley H, Hanson J. Changes in the cross-striations of muscle during contraction and stretch and their structural interpretation. Nature. 1954;173: 973–976.

20. Huxley AF, Niedergerke R. Structural changes in muscle during contraction; interference microscopy of living muscle fibres. Nature. 1954;173: 971–973.

21. Panner BJ, Honig CR. Filament ultrastructure and organization in vertebrate smooth muscle. Contraction hypothesis based on localization of actin and myosin. J Cell Biol. 1967;35: 303–321.

22. Hartman MA, Spudich JA. The myosin superfamily at a glance. J Cell Sci. 2012;125: 1627–1632.

23. Squire JM. General model for the structure of all myosin-containing filaments. Nature. 1971;233: 457–462.

24. Tang DD, Anfinogenova Y. Physiologic properties and regulation of the actin cytoskeleton in vascular smooth muscle. J Cardiovasc Pharmacol Ther. 2008;13: 130–140.

25. Gazzola M, Henry C, Lortie K, Khadangi F, Park CY, Fredberg JJ, et al. Airway smooth muscle tone increases actin filamentogenesis and contractile capacity. Am J Physiol Lung Cell Mol Physiol. 2020;318: L442–L451.

26. Ringer S. A further Contribution regarding the influence of the different Constituents of the Blood on the Contraction of the Heart. J Physiol. 1883;4: 29-42.3.

27. Liu X, Shu S, Korn ED. Polymerization pathway of mammalian nonmuscle myosin 2s. Proc Natl Acad Sci U S A. 2018;115: E7101–E7108.

28. Khalil RA, van Breemen C. Sustained contraction of vascular smooth muscle: calcium influx or C-kinase activation? J Pharmacol Exp Ther. 1988;244: 537–542.

29. Berridge MJ, Irvine RF. Inositol trisphosphate, a novel second messenger in cellular signal transduction. Nature. 1984;312: 315–321.

30. Lin Q, Zhao G, Fang X, Peng X, Tang H, Wang H, et al. IP3 receptors regulate vascular smooth muscle contractility and hypertension. JCI Insight. 2016;1: e89402.

31. de Lanerolle P, Stull JT. Myosin phosphorylation during contraction and relaxation of tracheal smooth muscle. J Biol Chem. 1980;255: 9993–10000.

32. Hafen BB, Burns B. Physiology, Smooth Muscle. StatPearls Publishing; 2022.

33. Heissler SM, Manstein DJ. Nonmuscle myosin-2: mix and match. Cell Mol Life Sci. 2013;70: 1–21.

34. Ogut O, Yuen SL, Brozovich FV. Regulation of the smooth muscle contractile phenotype by nonmuscle myosin. J Muscle Res Cell Motil. 2007;28: 409–414.

35. Mohammad MA, Sparrow MP. The distribution of heavy-chain isoforms of myosin in airways smooth muscle from adult and neonate humans. Biochem J. 1989;260: 421–426.

36. Morano I, Chai GX, Baltas LG, Lamounier-Zepter V. Smooth-muscle contraction without smooth-muscle myosin. Nat Cell Biol. 2000. Available: https://www.nature.com/articles/ncb0600_371

37. Morano I. Tuning smooth muscle contraction by molecular motors. J Mol Med. 2003;81: 481–487.

38. Yuen SL, Ogut O, Brozovich FV. Nonmuscle myosin is regulated during smooth muscle contraction. American Journal of. 2009. Available: https://journals.physiology.org/doi/abs/10.1152/ajpheart.00132.2009

39. Zhang W, Gunst SJ. Non-muscle (NM) myosin heavy chain phosphorylation regulates the formation of NM myosin filaments, adhesome assembly and smooth muscle contraction. J Physiol. 2017;595: 4279–4300.

40. Singh K, Kim AB, Morgan KG. Non-muscle myosin II regulates aortic stiffness through effects on specific focal adhesion proteins and the non-muscle cortical cytoskeleton. J Cell Mol Med. 2021. doi:10.1111/jcmm.16170

41. Holmes KC, Geeves MA. The structural basis of muscle contraction. Philos Trans R Soc Lond B Biol Sci. 2000;355: 419–431.

42. Lymn RW, Taylor EW. Mechanism of adenosine triphosphate hydrolysis by actomyosin. Biochemistry. 1971;10: 4617–4624.

43. Ni S, Hong F, Haldeman BD, Baker JE, Facemyer KC, Cremo CR. Modification of interface between regulatory and essential light chains hampers phosphorylation-dependent activation of smooth muscle myosin. J Biol Chem. 2012;287: 22068–22079.

44. Trybus KM, Freyzon Y, Faust LZ, Sweeney HL. Spare the rod, spoil the regulation: necessity for a myosin rod. Proc Natl Acad Sci U S A. 1997;94: 48–52.

45. Sellers JR. Myosins Oxford University Press. New York. 1999.

46. Jung HS, Billington N, Thirumurugan K, Salzameda B, Cremo CR, Chalovich JM, et al. Role of the tail in the regulated state of myosin 2. J Mol Biol. 2011;408: 863–878.

47. Milton DL, Schneck AN, Ziech DA, Ba M, Facemyer KC, Halayko AJ, et al. Direct evidence for functional smooth muscle myosin II in the 10S self-inhibited monomeric conformation in airway smooth muscle cells. Proc Natl Acad Sci U S A. 2011;108: 1421–1426.

48. Trybus KM, Huiatt TW, Lowey S. A bent monomeric conformation of myosin from smooth muscle. Proc Natl Acad Sci U S A. 1982;79: 6151–6155.

49. Suzuki H, Onishi H, Takahashi K, Watanabe S. Structure and function of chicken gizzard myosin. J Biochem. 1978;84: 1529–1542.

50. Hooijman P, Stewart MA, Cooke R. A new state of cardiac myosin with very slow ATP turnover: a potential cardioprotective mechanism in the heart. Biophys J. 2011;100: 1969–1976.

51. Alamo L, Ware JS, Pinto A, Gillilan RE, Seidman JG, Seidman CE, et al. Effects of myosin variants on interacting-heads motif explain distinct hypertrophic and dilated cardiomyopathy phenotypes. Elife. 2017;6: e24634.

52. Adelstein RS, Conti MA, Hathaway DR, Klee CB. PHOSPHORYLATON OF SMOOTH MUSCLE MYOSIN LIGHT CHAIN KINASE BY THE CATALYTIC SUBUNIT OF ADENOSINE 3′:5′-MONOPHOSPHATE DEPENDENT PROTEIN KINASE. In: Usdin E, Kopin IJ, Barchas J, editors. Catecholamines: Basic and Clinical Frontiers. Pergamon; 1979. pp. 992–994.

53. Adelstein RS, Conti MA. Phosphorylation of platelet myosin increases actin-activated myosin ATPase activity. Nature. 1975;256: 597–598.

54. Craig R, Smith R, Kendrick-Jones J. Light-chain phosphorylation controls the conformation

of vertebrate non-muscle and smooth muscle myosin molecules. Nature. 1983;302: 436–439.

55. Ikebe M, Hartshorne DJ, Elzinga M. Identification, phosphorylation, and dephosphorylation of a second site for myosin light chain kinase on the 20,000-dalton light chain of smooth muscle myosin. J Biol Chem. 1986;261: 36–39.

56. Sellers JR, Pato MD, Adelstein RS. Reversible phosphorylation of smooth muscle myosin, heavy meromyosin, and platelet myosin. J Biol Chem. 1981;256: 13137–13142.

57. Corson MA, Sellers JR, Adelstein RS, Schoenberg M. Substance P contracts bovine tracheal smooth muscle via activation of myosin light chain kinase. Am J Physiol. 1990;259: C258-65.

58. Rovner AS, Thompson MM, Murphy RA. Two different heavy chains are found in smooth muscle myosin. Am J Physiol. 1986;250: C861-70.

59. Babij P, Kelly C, Periasamy M. Characterization of a mammalian smooth muscle myosin heavy-chain gene: complete nucleotide and protein coding sequence and analysis of the 5' end of the gene. Proc Natl Acad Sci U S A. 1991;88: 10676–10680.

60. Somlyo AV, Somlyo AP. Electromechanical and pharmacomechanical coupling in vascular smooth muscle. J Pharmacol Exp Ther. 1968;159: 129–145.

61. Eddinger TJ, Meer DP. Single rabbit stomach smooth muscle cell myosin heavy chain SMB expression and shortening velocity. Am J Physiol Cell Physiol. 2001;280: C309-16.

62. Babu GJ, Warshaw DM, Periasamy M. Smooth muscle myosin heavy chain isoforms and their role in muscle physiology. Microsc Res Tech. 2000;50: 532–540.

63. Lauzon AM, Tyska MJ, Rovner AS, Freyzon Y, Warshaw DM, Trybus KM. A 7-amino-acid insert in the heavy chain nucleotide binding loop alters the kinetics of smooth muscle myosin in the laser trap. J Muscle Res Cell Motil. 1998;19: 825–837.

64. Léguillette R, Laviolette M, Bergeron C, Zitouni N, Kogut P, Solway J, et al. Myosin, transgelin, and myosin light chain kinase: expression and function in asthma. Am J Respir Crit Care Med. 2009;179: 194–204.

65. Boivin R, Vargas A, Lefebvre-Lavoie J, Lauzon A-M, Lavoie J-P. Inhaled corticosteroids modulate the (+)insert smooth muscle myosin heavy chain in the equine asthmatic airways. Thorax. 2014;69: 1113–1119.

66. Ikebe M, Hewett TE, Martin AF, Chen M, Hartshorne DJ. Cleavage of a smooth muscle myosin heavy chain near its C terminus by alpha-chymotrypsin. Effect on the properties of myosin. J Biol Chem. 1991;266: 7030–7036.

67. Eddinger TJ, Meer DP. Myosin isoform heterogeneity in single smooth muscle cells. Comp

Biochem Physiol B Biochem Mol Biol. 1997;117: 29–38.

68. Koretz JF. Structural studies of synthetic filaments prepared from column-purified myosin. Biophys J. 1979;27: 423–432.

69. Kaminer B, Szonyi E, Belcher CD. “Hybrid” myosin filaments from smooth and striated muscle. J Mol Biol. 1976;100: 379–386.

70. Liu X, Shu S, Korn ED. Muscle myosins form folded monomers, dimers, and tetramers during filament polymerization in vitro. Proc Natl Acad Sci U S A. 2020;117: 15666–15672.

71. Craig R, Megerman J. Assembly of smooth muscle myosin into side-polar filaments. J Cell Biol. 1977;75: 990–996.

72. Cooke PH, Fay FS, Craig R. Myosin filaments isolated from skinned amphibian smooth muscle cells are side-polar. J Muscle Res Cell Motil. 1989;10: 206–220.

73. Katayama E, Scott-Woo G, Ikebe M. Effect of caldesmon on the assembly of smooth muscle myosin. J Biol Chem. 1995;270: 3919–3925.

74. Kelley CA, Sellers JR, Goldsmith PK, Adelstein RS. Smooth muscle myosin is composed of homodimeric heavy chains. J Biol Chem. 1992;267: 2127–2130.

75. Tsao AE, Eddinger TJ. Smooth muscle myosin heavy chains combine to form three native myosin isoforms. Am J Physiol. 1993;264: H1653-62.

76. Wang G, Zhu Y, Li K, Liao B, Wang F, Shao L, et al. Curcumin-mediated photodynamic therapy inhibits the phenotypic transformation, migration, and foaming of oxidized low-density lipoprotein-treated vascular smooth muscle cells by promoting autophagy. J Cardiovasc Pharmacol. 2021. doi:10.1097/FJC.0000000000001069

77. Smolensky AV, Ragozzino J, Gilbert SH, Seow CY, Ford LE. Length-dependent filament formation assessed from birefringence increases during activation of porcine tracheal muscle. J Physiol. 2005;563: 517–527.

78. Kim HR, Gallant C, Leavis PC, Gunst SJ, Morgan KG. Cytoskeletal remodeling in differentiated vascular smooth muscle is actin isoform dependent and stimulus dependent. Am J Physiol Cell Physiol. 2008;295: C768-78.

79. Trybus KM. Filamentous smooth muscle myosin is regulated by phosphorylation. J Cell Biol. 1989;109: 2887–2894.

80. Sellers JR, Eisenberg E, Adelstein RS. The binding of smooth muscle heavy meromyosin to actin in the presence of ATP. Effect of phosphorylation. J Biol Chem. 1982;257: 13880–13883.

81. Rovner AS, Fagnant PM, Trybus KM. Phosphorylation of a single head of smooth muscle

myosin activates the whole molecule. Biochemistry. 2006;45: 5280–5289.

82. Walcott S, Fagnant PM, Trybus KM, Warshaw DM. Smooth muscle heavy meromyosin phosphorylated on one of its two heads supports force and motion. J Biol Chem. 2009;284: 18244–18251.

83. Breckenridge MT, Dulyaninova NG, Egelhoff TT. Multiple regulatory steps control mammalian nonmuscle myosin II assembly in live cells. Mol Biol Cell. 2009;20: 338–347.

84. Vicente-Manzanares M, Zareno J, Whitmore L, Choi CK, Horwitz AF. Regulation of protrusion, adhesion dynamics, and polarity by myosins IIA and IIB in migrating cells. J Cell Biol. 2007;176: 573–580.

85. Wood NB, Kelly CM, O'Leary TS, Martin JL, Previs MJ. Cardiac Myosin Filaments are Maintained by Stochastic Protein Replacement. Mol Cell Proteomics. 2022;21: 100274.

86. Webb RC. Smooth muscle contraction and relaxation. Adv Physiol Educ. 2003;27: 201–206.

87. Mody PS, Wang Y, Geirsson A, Kim N, Desai MM, Gupta A, et al. Trends in aortic dissection hospitalizations, interventions, and outcomes among medicare beneficiaries in the United States, 2000-2011. Circ Cardiovasc Qual Outcomes. 2014;7: 920–928.

88. Gao YZ, Saphirstein RJ, Yamin R, Suki B, Morgan KG. Aging impairs smooth muscle-mediated regulation of aortic stiffness: a defect in shock absorption function? Am J Physiol Heart Circ Physiol. 2014;307: H1252-61.

89. Zhu L, Vranckx R, Khau Van Kien P, Lalande A, Boisset N, Mathieu F, et al. Mutations in myosin heavy chain 11 cause a syndrome associating thoracic aortic aneurysm/aortic dissection and patent ductus arteriosus. Nat Genet. 2006;38: 343–349.

90. Imai Y, Morita H, Takeda N, Miya F, Hyodo H, Fujita D, et al. A deletion mutation in myosin heavy chain 11 causing familial thoracic aortic dissection in two Japanese pedigrees. Int J Cardiol. 2015;195: 290–292.

91. Takeda N, Morita H, Fujita D, Inuzuka R, Taniguchi Y, Nawata K, et al. A deleterious MYH11 mutation causing familial thoracic aortic dissection. Hum Genome Var. 2015;2: 15028.

92. Ravindra VM, Karsy M, Schmidt RH, Taussky P, Park MS, Bollo RJ. Rapid de novo aneurysm formation after clipping of a ruptured middle cerebral artery aneurysm in an infant with an MYH11 mutation. J Neurosurg Pediatr. 2016;18: 463–470.

93. Ardhanari M, Swaminathan S. Congenital ductus arteriosus aneurysm in association with MYH11 mutation: a case report. Cardiol Young. 2020;30: 123–125.

94. Das S, Zhang E, Senapati P, Amaram V, Reddy MA, Stapleton K, et al. A Novel

Angiotensin II-Induced Long Noncoding RNA Giver Regulates Oxidative Stress, Inflammation, and Proliferation in Vascular Smooth Muscle Cells. Circ Res. 2018;123: 1298–1312.

95. Lin C-J, Hunkins BM, Roth RA, Lin C-Y, Wagenseil JE, Mecham RP. Vascular Smooth Muscle Cell Subpopulations and Neointimal Formation in Mouse Models of Elastin Insufficiency. Arterioscler Thromb Vasc Biol. 2021;41: 2890–2905.

96. Wang J, Uryga AK, Reinhold J, Figg N, Baker L, Finigan A, et al. Vascular Smooth Muscle Cell Senescence Promotes Atherosclerosis and Features of Plaque Vulnerability. Circulation. 2015;132: 1909–1919.

97. Kimes BW, Brandt BL. Characterization of two putative smooth muscle cell lines from rat thoracic aorta. Exp Cell Res. 1976;98: 349–366.

98. Beach JR, Shao L, Remmert K, Li D, Betzig E, Hammer JA 3rd. Nonmuscle myosin II isoforms coassemble in living cells. Curr Biol. 2014;24: 1160–1166.

99. Miano JM, Fisher EA, Majesky MW. Fate and State of Vascular Smooth Muscle Cells in Atherosclerosis. Circulation. 2021;143: 2110–2116.

100. Rademacher DJ, Cabe M, Bakowska JC. Fluorescence Recovery after Photobleaching of Yellow Fluorescent Protein Tagged p62 in Aggresome-like Induced Structures. J Vis Exp. 2019. doi:10.3791/59288

101. Eddinger TJ, Meer DP. Myosin II isoforms in smooth muscle: heterogeneity and function. Am J Physiol Cell Physiol. 2007;293: C493-508.

102. White SL, Zhou MY, Low RB, Periasamy M. Myosin heavy chain isoform expression in rat smooth muscle development. Am J Physiol. 1998;275: C581-9.

103. DiSanto ME, Cox RH, Wang Z, Chacko S. NH2-terminal-inserted myosin II heavy chain is expressed in smooth muscle of small muscular arteries. Am J Physiol Cell Physiol. 1997;272: C1532–C1542.

104. Isotani E, Zhi G, Lau KS, Huang J, Mizuno Y, Persechini A, et al. Real-time evaluation of myosin light chain kinase activation in smooth muscle tissues from a transgenic calmodulin-biosensor mouse. Proc Natl Acad Sci U S A. 2004;101: 6279–6284.

105. Ojima K, Ichimura E, Yasukawa Y, Wakamatsu J-I, Nishimura T. Dynamics of myosin replacement in skeletal muscle cells. Am J Physiol Cell Physiol. 2015;309: C669-79.

106. Ojima K, Ichimura E, Yasukawa Y, Oe M, Muroya S, Suzuki T, et al. Myosin substitution rate is affected by the amount of cytosolic myosin in cultured muscle cells. Anim Sci J. 2017;88: 1788–1793.

107. Horváth ÁI, Gyimesi M, Várkuti BH, Képiró M, Szegvári G, Lőrincz I, et al. Effect of

allosteric inhibition of non-muscle myosin 2 on its intracellular diffusion. Sci Rep. 2020;10: 13341.

108. Sprague BL, Pego RL, Stavreva DA, McNally JG. Analysis of binding reactions by fluorescence recovery after photobleaching. Biophys J. 2004;86: 3473–3495.

109. Tang DD. The Dynamic Actin Cytoskeleton in Smooth Muscle. Adv Pharmacol. 2018;81: 1–38.

110. Shutova MS, Spessott WA, Giraudo CG, Svitkina T. Endogenous species of mammalian nonmuscle myosin IIA and IIB include activated monomers and heteropolymers. Curr Biol. 2014;24: 1958–1968.

111. Löfgren M, Ekblad E, Morano I, Arner A. Nonmuscle Myosin motor of smooth muscle. J Gen Physiol. 2003;121: 301–310.

112. Satoh H. Modulation of Ca2+-activated K+ current by isoprenaline, carbachol, and phorbol ester in cultured (and fresh) rat aortic vascular smooth muscle cells. General Pharmacology: The Vascular System. 1996;27: 319–324.

113. Elliott DF, Peart WS. Amino-acid sequence in a hypertensin. Nature. 1956;177: 527–528.

114. Alexander RW, Brock TA, Gimbrone MA Jr, Rittenhouse SE. Angiotensin increases inositol trisphosphate and calcium in vascular smooth muscle. Hypertension. 1985;7: 447–451.

115. Smolensky AV, Gilbert SH, Harger-Allen M, Ford LE. Inhibition of myosin light-chain phosphorylation inverts the birefringence response of porcine airway smooth muscle. J Physiol. 2007;578: 563–568.

116. Seawright JW, Sreenivasappa H, Gibbs HC, Padgham S, Shin SY, Chaponnier C, et al. Vascular Smooth Muscle Contractile Function Declines With Age in Skeletal Muscle Feed Arteries. Front Physiol. 2018;9: 856.

117. Nicholson CJ, Xing Y, Lee S, Liang S, Mohan S, O'Rourke C, et al. Ageing causes an aortic contractile dysfunction phenotype by targeting the expression of members of the extracellular signal-regulated kinase pathway. J Cell Mol Med. 2022;26: 1456–1465.

118. Kaess BM, Rong J, Larson MG, Hamburg NM, Vita JA, Levy D, et al. Aortic stiffness, blood pressure progression, and incident hypertension. JAMA. 2012;308: 875–881.

119. Kajuluri LP, Singh K, Morgan KG. Vascular aging, the vascular cytoskeleton and aortic stiffness. Explor Med. 2021;2: 186–197.

120. Vasan RS, Short MI, Niiranen TJ, Xanthakis V, DeCarli C, Cheng S, et al. Interrelations Between Arterial Stiffness, Target Organ Damage, and Cardiovascular Disease Outcomes. J Am Heart Assoc. 2019;8: e012141.

121. Fisher SA. Vascular smooth muscle phenotypic diversity and function. Physiol Genomics. 2010;42A: 169–187.

122. Hamada Y, Yanagisawa M, Katsuragawa Y, Coleman JR, Nagata S, Matsuda G, et al. Distinct vascular and intestinal smooth muscle myosin heavy chain mRNAs are encoded by a single-copy gene in the chicken. Biochem Biophys Res Commun. 1990;170: 53–58.

123. Seow CY. Myosin Crossbridge, Contractile Unit, and the Mechanism of Contraction in Airway Smooth Muscle: A Mechanical Engineer's Perspective. J Eng Sci Med Diagn Ther. 2019;2: 0108041–0108046.

124. Sobieszek IJ, Sobieszek A. Myosin assembly of smooth muscle: from ribbons and side polarity to a row polar helical model. J Muscle Res Cell Motil. 2022;43: 113–133.

125. Kelley MJ, Jawien W, Ortel TL, Korczak JF. Mutation of MYH9, encoding non-muscle myosin heavy chain A, in May-Hegglin anomaly. Nat Genet. 2000;26: 106–108.

126. Pal K, Nowak R, Billington N, Liu R, Ghosh A, Sellers JR, et al. Megakaryocyte migration defects due to nonmuscle myosin IIA mutations underlie thrombocytopenia in MYH9-related disease. Blood. 2020;135: 1887–1898.

VITA

The author, Maggie, was born in Wilmington, NC on December 16, 1992 to Paul and Patricia Bennett. She attended Boston college where she earned a Bachelor's of Science in Biological Sciences in May 2015, and Master's of Science in Biological Sciences in May 2016. After graduation, Maggie matriculated into the Loyola University Chicago Stritch School of Medicine MD/PhD combined program and began her graduate education in the Cell and Molecular Physiology department under the supervision of Dr. Jordan Beach.

After completion of her graduate studies, Maggie will continue medical school at Loyola.